A Section 508–conformant HTML version of this article is available at https://doi.org/10.1289/EHP8580.

Gene–Environment Interactions in Developmental Neurotoxicity: a Case Study of Synergy between Chlorpyrifos and CHD8 Knockout in Human BrainSpheres

Sergio Modafferi,[1,2] Xiali Zhong,[1,3]* Andre Kleensang,[1] Yohei Murata,[1,4] Francesca Fagiani,[1,5,6] David Pamies,[1,7] Helena T. Hogberg,[1] Vittorio Calabrese,[2] Herbert Lachman,[8,9] Thomas Hartung,[1,10] and Lena Smirnova[1]*

[1]Center for Alternatives to Animal Testing, Bloomberg School of Public Health, Johns Hopkins University, Baltimore, Maryland, USA
[2]Department of Biomedical and Biotechnological Sciences, School of Medicine, University of Catania, Catania, Italy
[3]Guangdong Provincial Key Laboratory of Food, Nutrition and Health, Department of Toxicology, School of Public Health, Sun Yat-sen University, Guangzhou, China
[4]Research Center, Nihon Nohyaku Co. Ltd., Osaka, Japan
[5]Department of Drug Sciences, Pharmacology Section, University of Pavia, Pavia, Italy
[6]Istituto Universitario di Studi Superiori (Scuola Universitaria Superiore IUSS) Pavia, Pavia, Italy
[7]Department of Biomedical Science, University of Lausanne, Lausanne, Switzerland
[8]Department of Psychiatry and Behavioral Sciences, Albert Einstein College of Medicine, Bronx, New York, USA
[9]Dominick P. Purpura Department of Neuroscience, Albert Einstein College of Medicine, Bronx, New York, USA
[10]University of Konstanz, Konstanz, Germany

Background: Autism spectrum disorder (ASD) is a major public health concern caused by complex genetic and environmental components. Mechanisms of gene–environment (G × E) interactions and reliable biomarkers associated with ASD are mostly unknown or controversial. Induced pluripotent stem cells (iPSCs) from patients or with clustered regularly interspaced short palindromic repeats and CRISPR-associated protein 9 (CRISPR/Cas9)-introduced mutations in candidate ASD genes provide an opportunity to study (G × E) interactions.

Objectives: In this study, we aimed to identify a potential synergy between mutation in the high-risk autism gene encoding chromodomain helicase DNA binding protein 8 (*CHD8*) and environmental exposure to an organophosphate pesticide (chlorpyrifos; CPF) in an iPSC-derived human three-dimensional (3D) brain model.

Methods: This study employed human iPSC-derived 3D brain organoids (BrainSpheres) carrying a heterozygote CRISPR/Cas9-introduced inactivating mutation in *CHD8* and exposed to CPF or its oxon-metabolite (CPO). Neural differentiation, viability, oxidative stress, and neurite outgrowth were assessed, and levels of main neurotransmitters and selected metabolites were validated against human data on ASD metabolic derangements.

Results: Expression of CHD8 protein was significantly lower in *CHD8* heterozygous knockout ($CHD8^{+/-}$) BrainSpheres compared with $CHD8^{+/+}$ ones. Exposure to CPF/CPO treatment further reduced CHD8 protein levels, showing the potential (G × E) interaction synergy. A novel approach for validation of the model was chosen: from the literature, we identified a panel of metabolic biomarkers in patients and assessed them by targeted metabolomics *in vitro*. A synergistic effect was observed on the cholinergic system, *S*-adenosylmethionine, *S*-adenosylhomocysteine, lactic acid, tryptophan, kynurenic acid, and α-hydroxyglutaric acid levels. Neurite outgrowth was perturbed by CPF/CPO exposure. Heterozygous knockout of *CHD8* in BrainSpheres led to an imbalance of excitatory/inhibitory neurotransmitters and lower levels of dopamine.

Discussion: This study pioneered (G × E) interaction in iPSC-derived organoids. The experimental strategy enables biomonitoring and environmental risk assessment for ASD. Our findings reflected some metabolic perturbations and disruption of neurotransmitter systems involved in ASD. The increased susceptibility of $CHD8^{+/-}$ BrainSpheres to chemical insult establishes a possibly broader role of (G × E) interaction in ASD. https://doi.org/10.1289/EHP8580

Introduction

Autism spectrum disorder (ASD) includes a cluster of neurodevelopmental conditions characterized by variable deficits in social communication and interaction, as well as restricted, stereotyped, and repetitive interests and behaviors (Lai et al. 2014; Mandy and Lai 2016). Individuals with ASD may show a broad range of comorbidities: epilepsy, attention deficits, intellectual disability, gastrointestinal problems, and diverse motor cognitive and mood impairments—all of which contribute to clinical heterogeneity (Courchesne et al. 2019). ASD is a major public health concern given that its prevalence is currently estimated at ∼1.5% in developed countries (Baxter et al. 2015; Lyall et al. 2017).

Recent developments in imaging and genetic techniques have led to significant advances in the understanding of ASD and paved the way for new approaches to study its pathophysiology. For instance, genome-wide association and large-scale sequencing studies have identified hundreds of ASD risk loci with common and rare risk variants, highlighting the heterogeneity of ASD genetic contribution (De Rubeis et al. 2014; Sanders 2015; Sanders et al. 2015; Satterstrom et al. 2020; Vorstman et al. 2017; Willsey et al. 2013). High-confidence genes were identified and predicted to be involved in pathways affected in ASD (Ayhan and Konopka 2019). Overall genetic effects, however, account for ∼59% of the etiological contribution to ASD, leaving a substantial role for environment-mediated effects (Gaugler et al. 2014). It is now generally believed that diverse (epi)genetic factors, environmental factors, and gene–environment (G × E) interactions increase autism risk (Chaste and Leboyer 2012; Dietert et al. 2011; Karimi et al. 2017; Kim et al. 2019; Koufaris and Sismani 2015; LaSalle 2013; Lyall et al. 2017; Modabbernia et al. 2017; Peter et al. 2015; Rossignol et al. 2014). How environmental factors and genetic susceptibilities interact to increase ASD risk remains mostly unknown.

For many years, autism research relied largely on animal models (Halladay et al. 2009). Rodent and human brain development,

*These authors contributed equally to this work.

Address correspondence to Lena Smirnova, 615 N. Wolfe St., W7032, Baltimore, MD 21205 USA. Telephone: (410) 614-4890. Email: lena.smirnova@jhu.edu

Supplemental Material is available online (https://doi.org/10.1289/EHP8580).

T.H., H.T.H., and D.P. are named inventors on a patent by Johns Hopkins University on the production of mini-brains (also called BrainSpheres), which is licensed to AxoSim, New Orleans, Louisiana, USA. T.H., L.S., D.P., and H.T.H. are consultants for AxoSim, New Orleans, and T.H. is also a consultant for AstraZeneca and American Type Culture Collection (ATCC) on advanced cell culture methods. All other authors declare they have no actual or potential competing financial interests.

Received 29 October 2020; Revised 31 May 2021; Accepted 4 June 2021; Published 14 July 2021.

Note to readers with disabilities: *EHP* strives to ensure that all journal content is accessible to all readers. However, some figures and Supplemental Material published in *EHP* articles may not conform to 508 standards due to the complexity of the information being presented. If you need assistance accessing journal content, please contact ehponline@niehs.nih.gov. Our staff will work with you to assess and meet your accessibility needs within 3 working days.

however, differ significantly (Lancaster et al. 2013; Rice and Barone 2000). Although useful for morphological/phenotypical and behavioral studies, animal-based models for neurological disorders have shown limitations in modeling human disease and efficacy of interventions. One example is Alzheimer's disease, with a failure rate of 99.6% in drug discovery (Mohs and Greig 2017; Pistollato et al. 2016). In general clinical trials, success rates for neurological disorders were half the rate of other indications (Butlen-Ducuing et al. 2016). For ASD, in the absence of drug trials, no such direct comparisons are possible. A human-relevant model promises to find (G × E) interactions, particularly for the study of molecular mechanisms of those interactions and biomarkers of disease and to complement animal behavioral studies. Advantages of stem cell-derived test systems, whether two- (2D) or three-dimensional (3D), over traditional animal models include *a*) enabling the generation of human disease-relevant cell types; *b*) leveraging the genetic background of interest, either from patients or introduced by gene editing; and *c*) employing those cell types for medium- to high-throughput screening for toxicants and drugs because cellular models require less time and costs. Simple monolayer *in vitro* models, however, do not represent human organ function, have limited shelf-lifes, and lack the complexity of *in vivo* structure and physiology. Therefore, more complex systems that better mimic human brain architecture and function are needed (Astashkina and Grainger 2014; Marx et al. 2016, 2020; Pamies and Hartung 2017). Emerging 3D human organoid-based culture systems (especially those derived from iPSCs), promise the possibility of (G × E) interaction testing at the cellular and molecular levels in human-relevant models (Yang and Shcheglovitov 2020). 3D iPSC-derived neural cultures better recapitulate key events of neural development (neural and glial differentiation, migration, myelination, and synaptogenesis) than monolayer models do (Limongi et al. 2013). 3D neural cultures show increased survival and enhanced neural differentiation compared with traditional 2D cultures (Peretz et al. 2007; Brännvall et al. 2007), allowing them to reach the later stages of neurodevelopment, where they can be differentiated into astrocytes and oligodendrocytes. Thus, the 3D systems have more heterogeneous *in vivo*-relevant cellular composition compared with the more homogeneous single-cell–type 2D cultures. A prolonged shelf-life is also beneficial in studies of the long-term and delayed effects of toxicants. The clustered regularly interspaced short palindromic repeats and CRISPR-associated protein 9 (CRISPR/Cas9) genome-editing of iPSCs further strengthens these models by enabling the generation of gain- and loss-of-function mutations in genes of interest, greatly facilitating the interpretation of risk allele effects on neuronal function (Wang et al. 2017).

ASD susceptibility genes converge during certain periods in development and on specific biological pathways, including those for transcription/chromatin remodeling complexes and synaptic function (Modabbernia et al. 2017). Data are accumulating on environmental chemicals that potentially interact with these signaling pathways (Stamou et al. 2013). Loss-of-function mutations in regulator genes can initiate developmental network dysregulations and cause ASD (Ayhan and Konopka 2019). The *CHD8* gene is an example of a high-risk ASD gene (Cotney et al. 2015; Neale et al. 2012; Stolerman et al. 2016). CHD8 is an ATP-dependent protein that represses transcription by altering nucleosome positioning and regulates a network of genes critical for early neurodevelopment (Bernier et al. 2014). Studies in human samples (Bernier et al. 2014), as well as in cellular (Wang et al. 2015; Cotney et al. 2015; Sugathan et al. 2014) and animal (Cotney et al. 2015) models, demonstrated that *CHD8* mutations modulate other genes involved in ASD, affecting global development, neural differentiation, and brain volume. Results with cerebral organoids derived from iPSCs with a *CHD8* null mutation, for example, showed that CHD8 can affect GABAergic interneuron development consistent with abnormalities in cortical gamma-aminobutyric acid (GABA) interneuron function found in a subgroup of ASD (Wang et al. 2017).

Organophosphorus pesticides (OPs), such as chlorpyrifos (CPF), are widely used in agriculture, with consequent exposures of workers and residents of agricultural communities, as well as the general population through consumption of OP-treated agricultural products (Rauh et al. 2012). However, there is a vast literature reporting their adverse effects on the developing nervous system (Juberg et al. 2019; Mie et al. 2018; Rauh et al. 2006; Stamou et al. 2013). Several epidemiological (Rauh et al. 2011, 2012; Eaton et al. 2008) and animal studies (De Felice et al. 2016; Eaton et al. 2008) have showed that developmental exposure to CPF, even at subtoxic levels, has adverse effects on brain maturation—targeting pathways involved in ASD etiology—and may induce various neurobehavioral deficits as well as structural abnormalities (such as thinning of the cerebral cortex) (Grandjean and Landrigan 2014). In addition, exposure of mothers to CPF during the second trimester of pregnancy has been associated with a higher risk of ASD in their children (Shelton et al. 2014).

Although the mechanism underlying the risk of ASD from OP exposure is unknown, it has been suggested that OPs could affect the expression and function of ASD risk genes and derail normal neurodevelopment. Whether there exists a particularly vulnerable subpopulation at greater risk for pesticide exposure remains to be clarified using (G × E) interaction studies (Stamou et al. 2013). Establishing clear associations between environmental and genetic ASD risk factors, however, could be particularly challenging, considering the extremely heterogeneous genetics of ASD and the susceptibility of the developing brain to multiple environmental insults. Our approach, therefore, aimed to identify and study interactions/synergies between one specific environmental factor and ASD risk gene. Identified synergies may point out the signaling pathways relevant for ASD, which can be potentially dysregulated by both. This might establish a role for (G × E) interaction in ASD that could be expanded to other developmental neurotoxicants and risk genes.

In the present study, we aimed to address the (G × E) interaction hypothesis in ASD by using an iPSC-derived brain organoid model with CRISPR/Cas9-engineered *CHD8* heterozygous knockout (*CHD8*$^{+/-}$ BrainSpheres) and exposure to CPF. To account for limiting xenobiotic metabolism *in vitro*, the active metabolite chlorpyrifos-oxon (CPO), which actively inhibits acetylcholinesterase (AChE) (Koshlukova and Reed 2014)—a primary acute mode of action among OPs—was also included. A literature survey identified adverse outcome pathways (AOPs) and an array of putative biomarkers of metabolic perturbation in individuals with ASD, which were then analyzed in BrainSpheres, with or without an ASD genetic background, exposed to CPF and CPO. The present study demonstrates the usefulness of an approach comparing human data with data obtained *in vitro* to identify possible biomarkers of exposure, as well as to identify ASD-relevant molecular networks perturbed by chemical exposure.

Methods

BrainSphere Differentiation

CHD8$^{+/+}$ and *CHD8*$^{+/-}$ neural progenitor cells (NPCs) were generated earlier from the *iPS-2C1* and *iPS-2C4G1C4* lines, respectively, authenticated and characterized by H.L.'s group (Wang et al. 2015, 2017). Frozen stocks of the NPCs were transferred to Johns Hopkins, where the main experiments were conducted. Upon receipt, NPCs were tested for mycoplasma contamination by the polymerase chain reaction (PCR)-based MycoDtect kit (Greiner Bio-One) at Johns Hopkins Genetics Resources Core Facility (tests were reported as negative). NPCs were expanded in poly L-ornithine and

laminin-coated 175-cm^2 flasks in NPC medium [KnockOut Dulbecco's Modified Essential Medium/Ham's F-12 Medium, 5% penicillin-streptomycin (Pen/Strep), 1× Stempro, 2× glutamax, 0.02 μg/mL human basic fibroblast growth factor, and 0.02 μg/mL human epidermal growth factor]—all reagents were from Thermo Fisher Scientific. Cells were maintained at 37°C, 5% carbon dioxide. Half of the medium was changed daily.

CHD8$^{+/+}$ and *CHD8*$^{+/-}$ BrainSphere differentiation followed our previously published protocol without any modifications (Pamies et al. 2017). Briefly, 2×10^6 NPCs were plated per well in noncoated 6-well plates and cultured under constant gyratory shaking (88 rpm, 19 mm orbit) in NPC medium. After 48 h, the medium was changed to differentiation medium [Neurobasal electro Medium (Thermo Fisher Scientific), 5% Pen/Strep, 2× glutamax, 1× B-27 electro (Gibco; Thermo Fisher Scientific), 0.01 μg/mL human glial cell line-derived neurotrophic factor (GeminiBio), and 0.01 μg/mL human brain-derived neurotrophic factor (GeminiBio)]. Cultures were maintained under constant gyratory shaking for up to 8 wk. Differentiation medium was exchanged every second day. The neural differentiation efficiency was assessed by immunocytochemistry (Figure 1B; Figure S1) and real-time PCR (RT-PCR) (Figure S2).

CPF and CPO Treatment, Cytotoxicity Assay

100 mM stocks of CPF and CPO (Sigma-Aldrich) were made in dimethyl sulfoxide (DMSO), aliquoted, and stored at −20°C. For all experiments, BrainSpheres were exposed to 100 μM CPF or CPO for 24 h at 4 wk of differentiation. The high concentrations and short-term exposures employed do not suggest a risk to humans in the real world, but were rather used as a model exposure, making use of the substance's well-established developmental neurotoxic (DNT) hazard (as described above in the "Introduction" section). For viability testing, an 8-wk time point was included, as well as a CPF/CPO concentration of 47 μM. DMSO (<0.01%) was used as vehicle control. Four weeks was selected as the intermediate, immature stage of differentiation, during which the main types of neurons are present but are still further maturating, the first astroglia and oligodendrocytes are emerging (as demonstrated by Pamies et al. 2017). Between 4 and 8 wk, expression of mature neural markers further increased. At 8 wk, BrainSpheres represented cultures of more mature neurons and glial cells with a low percentage of NPCs (Figures S1 and S2). For viability measurements, BrainSpheres were equally distributed in a 24-well plate for 24-h exposure without shaking (one 6-well into four wells of a 24-well plate, which is around 30 BrainSpheres per well). Four- and 8-wk spheroids were exposed to vehicle, 47 and 100 μM CPF, or its oxon (i.e., CPO). After 24-h exposure, the resazurin reduction assay was performed (Harris et al. 2017). Viability was measured using a multiwell fluorometric reader CytoFluor series 4000 (Perspective Biosystems) in three independent experiments (two for CPO-treated spheroids at 8-wk time point), with six to nine technical replicates in total.

Measurement of Mitochondria Membrane Potential and Reactive Oxygen Species

Mitochondrial membrane potential (MMP) was assessed using MitoTracker Red CMXROX (Thermo Fisher Scientific) and images were taken with an ECHO laboratories Revolve microscope with 4/0.13 magnification objective and quantified with ImageJ (Schneider et al. 2012) as previously described in detail (Harris et al. 2017). MMP was assessed in at least seven spheroids per condition/per experiment in three independent experiments. Production of reactive oxygen species (ROS) was assessed by CellROX Green Reagent (Thermo Fisher Scientific) and quantified by flow cytometry. Briefly, BrainSpheres were treated with 5 μM CellROX Green reagent for 45 min. Spheroids were washed three times with Hibernate E medium (Gibco) and dissociated with Collagenase IV/Papain/DNAse to a single-cell suspension as described in (Fan et al. 2018). Levels of ROS were measured on a BD LSRII flow cytometer using Diva software. Unstained cells were used for gating. Data from three independent experiments were analyzed with FlowJo (version 10.4.2; FlowJo LLC, Becton Dickinson, https://www.flowjo.com/solutions/flowjo) and presented as means ± standard errors of the mean (SEMs).

RNA Extraction and RT-PCR

Total RNA was extracted using Trizol (Thermo Fisher Scientific) and concentrated using an RNA clean and concentrator kit (Zymo Research). RNA quantity and purity were determined using NanoDrop 2000c. Five hundred nanograms of RNA was reverse-transcribed using M-MLV Reverse Transcriptase and Random Hexamer primers (Promega) according to the manufacturer's instructions. The expression of genes was evaluated using the TaqMan gene expression assay (Applied Biosystems) or SYBRGreen assay (listed in Tables S1 and S2). Real-time quantitative PCR (RT-qPCR) was performed using a 7500 Fast Real-Time system machine (Applied Biosystems). The genes for glyceraldehyde-3-phosphate dehydrogenase (*GAPDH*) or *18S* were used as housekeeping genes. To demonstrate gene expression levels during differentiation, RT-PCR results were presented as $2^{-\Delta Ct}$. Fold changes were calculated using the $2^{-\Delta\Delta Ct}$ method if gene expression was compared between treated and control samples and between cell lines. All $2^{-\Delta\Delta Ct}$ values were normalized to vehicle-treated controls of the *CHD8*$^{+/+}$ cell line and underwent $\log_2$ transformation. Means ± SEMs from at least four independent experiments (with 5 to 16 technical replicates in total) were calculated.

Immunofluorescence Staining of the BrainSpheres

BrainSpheres were fixed with 2% paraformaldehyde solution for 45 min and blocked for 2 h with 0.15% saponin (Millipore), 5% normal goat serum and 1% bovine serum albumin at room temperature. The spheres were then stained with primary antibodies (Table S3) for 48 h and with secondary antibodies (Table S4) for 24 h in blocking solution at 4°C, as described by Harris et al. (2017). Nuclei were stained with Hoechst 33342. BrainSpheres were mounted on glass slides. Images were taken using a Zeiss UV-LSM 700 confocal microscope with 20× and 63× magnification objectives and Zeiss Zen software (https://www.zeiss.com/microscopy/us/products/microscope-software/zen-lite.html).

Measurement of Acetylcholinesterase E Activity

The acetylcholinesterase (AChE) assay (Abcam; ab138873) was performed according to the manufacturer's instructions. Briefly, spheroids were lysed in lysis buffer (0.3 g sodium chloride; 1 mL of 1 M Tris, pH 7.5; 1 mL 10% NP-40; 0.2 mL of 0.5 M ethylenediaminetetraacetic acid, pH 8.0; 17.8 mL double-distilled water) and centrifuged at 600× *g* for 5 min. Fifty microliters of supernatant was combined with 50 μL of assay buffer in a 96-well plate and incubated for 20 min in the dark. The reaction was stopped with stop buffer. The fluorescence was measured at 540 nm using a multiwell fluorometric reader CytoFluor series 4000 (Perspective Biosystems). AChE activity was measured in three independent experiments.

Neurite Outgrowth

The detailed protocol of neurite outgrowth was published previously (Harris et al. 2018, 2017; Zhong et al. 2020). Briefly, after exposure to CPF/CPO, spheroids were plated in Matrigel-coated 24-well black glass-bottom plates (Cellvis) and incubated without shaking for 24–48 h to allow outgrowth of neurites. Spheroids were then immunostained with β-III-tubulin antibody as described above. Spheroids were imaged with a Zeiss LSM 500 confocal microscope with a 10× magnification objective (Figure 3; Figures S5 and S6) or with an ECHO laboratories Revolve microscope with 4/0.13 magnification objective (Figures S5–S7). Neurite density and length were quantified using the ImageJ Sholl plug-in for each individual spheroid. The ratio was calculated for each shell (number of intersections/distance from the edge of the spheroid) and plotted. The area under the curve (AUC) was calculated for each spheroid and then averaged. The experiment was repeated three times. To attenuate the CPF effect on neurite outgrowth, the BrainSpheres were pretreated with 100 μM tocopherol 2 h prior to CPF exposure.

Western Blot Analysis

Western blots were performed as described by Zhong et al. (2020). Briefly, spheroids were lysed with radioimmunoprecipitation assay lysis buffer (Sigma-Aldrich). Protein concentration was quantified with NanoDrop 2000c and the bicinchoninic acid (BCA) kit (both from Thermo Fisher Scientific). Lysates were separated on 4–15% gradient sodium dodecyl sulfate–polyacrylamide gels at 100 V for 120 min and transferred to a polyvinylidene difluoride membrane by electroblotting for 120 min at 200 mA and 4°C. After 1 h of blocking with blocking solution (phosphate-buffered saline; 0.5% Tween-20, pH 7.4, containing 5% nonfat dry milk), the membranes were incubated with primary antibodies [CHD8 (Cell Signaling; 7656S, 1:1,000); GAPDH (Cell Signaling; 2118S, 1:1,000)] overnight at 4°C, followed by washing and secondary antibody incubation for 1 h (horseradish peroxidase-conjugated antimouse, 1:3,000, antirabbit 1:2,000; BIO-RAD). The protein of interest was detected by chemiluminescence reagent (BIO-RAD; Clarity Western ECL Substrate) and exposed to film. Quantification was performed using Image-J (Schneider et al. 2012) software. Data was normalized to vehicle-treated *CHD8*$^{+/+}$ BrainSpheres and presented as means ± SEMs from five independent experiments.

Liquid Chromatography/Tandem Mass Spectrometry

For liquid chromatography/tandem mass spectrometry (LC-MS/MS) analysis, the BrainSpheres were lysed in 100% methanol/0.1% formic acid/3,4-dihydroxybenzylamine (Sigma-Aldrich) as spike-in, and subsequently sonicated twice for 2 min. Lysates were centrifuged at 25,000 × *g* for 30 min at 4°C. The supernatant was transferred to a new tube and 10-μL aliquots were taken for protein quantification using the BCA kit (Thermo Fisher Scientific). Samples were dried for at least 6 h in a SpeedVac at 35°C and reconstituted in 0.1% formic acid in water/acetonitrile (50:50).

LC–MS/MS was run on an Agilent 6490A triple-stage quadrupole MS equipped with a Jet Stream electrospray ionization ion source and a 1260 high-performance LC system. The analytes were separated at 35°C on a Sigma Discovery HS F5 column in reverse phase (150 × 2.1 mm, 3 μm) or an Agilent Poroshell 120 hydrophilic interaction liquid chromatography-zwitterionic (HILIC-Z), PEEK-lined (150 × 2.1 mm, 2.7 μm) in normal phase, depending on retention time of the metabolite. The mobile phase [0.1% formic acid in water (Solvent A) and 98% acetonitrile plus 0.1% formic acid (Solvent B)] was used with a gradient elution. For reverse phase, Solvent B was used at a flowrate of 0.3 mL/min. First, 0% Solvent B was used for 0–3 min, then 100% Solvent B for 23 min. For normal-phase HILIC, 92% Solvent B was used for 0–3 min, followed by 61% Solvent B for 23 min at a flowrate of 0.25 mL/min. It was necessary to use benzoyl chloride derivatization for some of the metabolites to increase sensitivity and stability of metabolite detection. Briefly, samples were dried and resuspended in freshly prepared reaction buffer consisting of 1 vol% benzoyl chloride, 50 vol% sodium tetraborate buffer, and 49 vol% acetonitrile. After incubation at 50°C for 30 min, the reaction was stopped by adding formic acid to a final concentration of 0.7 vol%. Metabolomics quality assurance followed recommendations by Beger et al. (2019) and Bouhifd et al. (2015). In brief, all metabolites were identified, transitions and retention times established, and the measurements optimized as a spike-in (3,4-dihydroxybenzylamine) reference metabolites in a quality control (QC) mixture of various samples from the same study. Each measurement run also consisted of blank cell culture media extractions to measure background levels (if appropriate) and two samples with spike-in reference metabolites in a QC-mixture of all samples of the corresponding run to address possible retention time drifts. MS transmission and quadruple tuning were checked before and after each run, and LC-MS/MS was regularly maintained following the recommendations of the manufacturer.

Peaks were integrated with the Agilent MassHunter WorkStation Quantitative Analysis software (version 10.1). All peaks were manually checked and integration was corrected if necessary. The AUC for each peak was normalized on the protein content in each sample and spike-in control (when included). The glutamate/GABA and *S*-adenosylmethionine/*S*-adenosylhomocysteine (SAM/SAH) ratios were calculated as follows: AUC(glutamate)/AUC(GABA) and AUC(SAM)/AUC(SAH), respectively. All metabolites were measured in two batches (Neuro1 and Neuro2; Table S5). In total, 1,536 measurements were conducted, in which 65 (4%) failed, and those outliers were replaced by an average of the technical replicates from the same experiment. The following outliers were identified: *a*) in Neuro1 and Neuro2 batches, two samples [*CHD8*$^{+/-}$ CPO2 (run 2) and *CHD8*$^{+/+}$ CPO2 (run 3) were excluded due to the error in protein quantification]; *b*) no peak was detected for all tested metabolites in two samples *CHD8*$^{+/+}$ DMSO1 and *CHD8*$^{+/-}$ CPO1 (run 3) due to a technical error during the derivatization experiment of Neuro1 batch; *c*) two DMSO controls in *CHD8*$^{+/+}$ Neuro2 batch measurement had significant lower peaks than the rest of the samples due to the sample being dried out; *d*) no peak was detected for cysteine in one sample [*CHD8*$^{+/+}$ CPF2 (run 2)]; and *e*) CHD8$^{+/-}$ CPF2 and CHD8$^{+/-}$ CPO 2 (run 3) were identified as outliers for folic acid and sample CHD8$^{+/-}$ CPF5 (run 2)—for the cysteine/cystine ratio by visual inspection of Tukey's box-and-whiskers plots and robust regression and outlier removal function in GraphPad (version 9.1) software. The LC-MS/MS experiment was repeated three times, with 12 technical replicates in total. Kynurenic acid and L-Cysteine, where measured in two experiments (8 technical replicates). All metabolites were then normalized to vehicle-treated *CHD8*$^{+/+}$ samples.

Literature Search of ASD-Relevant Metabolites in Human Blood, Urine, and Brain Samples

A literature review of the articles published before 1 May 2020 was conducted in PubMed and Google Scholar. The search terms used were "metabolites" OR "amino acids" OR "neurotransmitters" OR "metabolomics" OR "metabolomic analysis" AND "autism" OR "autism spectrum disorder." In addition, for each metabolite included in our metabolomic analysis, a search with "name of the metabolite" AND "autism" OR "autism spectrum disorder" was performed. Only population studies looking for metabolites in blood/serum, urine, or brain tissue and published in peer-reviewed journals were included.

Statistical Analysis

A detailed description of the statistical analysis is provided in each corresponding figure legend. Briefly, all assays were conducted in at least three independent experiments. If not specified otherwise, the data are presented as Tukey's box-and-whiskers plots showing quartiles with outliers. Numeric data (mean, SD, SEM, and N) were included either in the figures or in supplemental tables corresponding to the graphs. In order to compare different treatment groups between the cell lines in viability, AChE activity, Western blot, Mitotracker, CellRox, gene expression, and metabolomics experiments, a two-way analysis of variance (ANOVA) with posttest for multiple comparisons by the two-stage linear step-up procedure of Benjamini, Krieger, and Yekutieli and a desired false discovery rate of 0.01 (metabolomics and AChE activity) and 0.05 for the rest of the assays was used (Benjamini et al. 2006). To avoid further loss of statistical power, only the following post hoc tests were conducted for pairwise comparison between the groups: *a*) all samples were compared with *CHD8*$^{+/+}$ DMSO; *b*) CPF and CPO exposures were compared with corresponding vehicle controls within the genetic groups; *c*) vehicle controls and CPF/CPO exposures were compared between the *CHD8*$^{+/+}$ and *CHD8*$^{+/-}$ (DMSO vs. DMSO, CPF vs. CPF, and CPO vs. CPO). Statistical significance in neurite outgrowth experiment within the *CHD8*$^{+/+}$ and *CHD8*$^{+/-}$ groups was analyzed with a one-way ANOVA employing Holm-Sidak's multiple comparison test. A level of $p < 0.05$ was considered significant.

Results

Efficiency of BrainSphere Differentiation from CHD8$^{+/+}$ *and CHD8*$^{+/-}$ *NPC*

The control iPSC line (*CHD8*$^{+/+}$) and the iPSC line carrying a CRISPR/Cas9-induced heterozygous knockout mutation in the *CHD8* gene (*CHD8*$^{+/-}$) used in this study were generated from the same donor, differentiated into NPCs, and fully characterized previously (Wang et al. 2015, 2017). The *CHD8*$^{+/-}$ line is heterozygous for a two-base pair deletion, which leads to a frameshift mutation and premature stop signal in Exon 1. A lower level of CHD8 protein in CHD8$^{+/-}$ neuroprogenitors vs. CHD8$^{+/+}$ was confirmed and is shown in Figure 1A. Figure 1B shows immunostaining of control and CHD8$^{+/-}$ NPCs with the neuroprogenitor markers Sox2 and Nestin. Both NPC cell lines were differentiated to generate 3D BrainSphere cultures, as described in Figure 1C. We were not able to generate BrainSpheres from a homozygous *CHD8* knockout line (*CHD8*$^{-/-}$). The differentiation efficiency was compared between the two cell lines by immunostaining (Figure S1) and RT-PCR (Figure S2; Table S6). The BrainSpheres from both cell lines contained NPCs (Nestin^{+}, Ki-67^{+}), neurons (β-III-tubulin^{+}), neurofilament 200-positive (NF-200^{+}), microtubule-associated protein-2-positive (MAP2^{+}), astrocytes [glial fibrillary acidic protein-positive (GFAP^{+})], and oligodendrocytes [Olig1^{+}, myelin basic protein (MPB^{+})]. Co-immunostaining of neurons (β-III-tubulin^{+}, MAP2^{+}) with neuroprogenitors (Nestin^{+}, Ki-67^{+}) at 2, 4, and 8 wk of differentiation showed a progressive increase of β-III-tubulin^{+} and MAP2^{+} as well as a decrease of Nestin^{+} and Ki-67^{+} cells (Figure S1A,B), demonstrating neuronal maturation. GFAP^{+} astroglia, as well as Olig1^{+} and MBP^{+} oligodendroglia, were identified. Oligodendrocyte-specific markers were first expressed at high levels at 8 wk of differentiation (Figure S1C). Notably, *CHD8*$^{+/-}$ spheroids were slightly larger in diameter than *CHD8*$^{+/+}$ spheroids (Figure S1D).

At the gene expression level, a panel of neural genes—along with a set of autism risk genes and CHD8 targets—were analyzed by RT-PCR, which confirmed the similar efficiency of neural differentiation in both cell lines. Strong reduction in expression of progenitor marker genes (*Pax6, Sox2,* and *Ki-67*) and induction of neuronal (*β-III-Tubulin, NeuN, Synapsin1, AChE, GABRA1, RNXN2, SHANK3*) and glial (*GFAP*) genes were observed in the course of differentiation of both cell lines (Figure S2; Table S6).

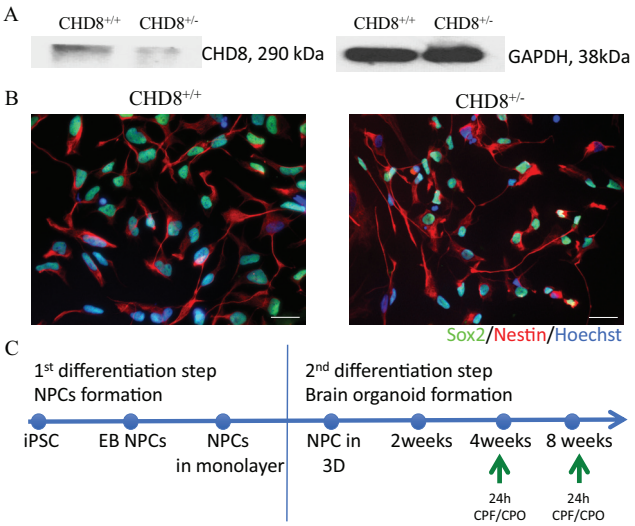

Figure 1. *CHD8*$^{+/+}$ and *CHD8*$^{+/-}$ NPC characterization. Scheme of BrainSphere differentiation. Prior differentiation to BrainSpheres, NPCs were expanded in monolayers and characterized. (A) CHD8 protein levels in *CHD8*$^{+/-}$ vs. *CHD8*$^{+/+}$ NPCs analyzed by western blot. (B) Representative images showing expression of the NPC markers Sox2 (green) and Nestin (red) in *CHD8*$^{+/+}$ and *CHD8*$^{+/-}$ NPC cultures prior to induction of differentiation into BrainSpheres. The nuclei were visualized with Hoechst 33342. Scale bar: 50 μm. (C) Differentiation and toxicant treatment scheme. Note: CPF, chlorpyrifos; CPO, oxon-metabolite of chlorpyrifos; EB, embryoid bodies; NPC, neural progenitor cell; 3D, three dimensional.

Several genes, however, showed different expression levels between *CHD8*$^{+/-}$ and *CHD8*$^{+/+}$ BrainSpheres. In agreement with previous studies (Wang et al. 2015, 2017), we observed higher expression of genes involved in GABAergic neuronal fate. *DLX1*, a transcription factor known to regulate GABAergic interneuron development, had higher expression in *CHD8*$^{+/-}$ BrainSpheres. Glutamate decarboxilase 1 (*GAD1*), a catalizer of GABA producation form glutamic acid, was higher in *CHD8*$^{+/-}$ NPC cultures (not significant). Expression of *GABRA1*, a marker for GABAergic neurons, was low in 2- and 4-wk BrainSpheres, but it was strongly up-regulated at 8 wk of differentiation, with higher expression in *CHD8*$^{+/-}$ BrainSpheres in comparison with the control cell line. *FOXG1*, another transcription factor responsible for GABAergic neuronal differentiation and telencephalon development, was, however, expressed at a similar level in both cell lines.

Postsynaptic *Neuroligin 3* (*NLGN3*) was expressed at higher levels at 8 wk in *CHD8*$^{+/-}$ BrainSpheres, whereas *SHANK3* did not show significant differences. Two other CHD8 targets and autism risk genes, *AUTS2* and *POGZ,* showed differing expression in *CHD8*$^{+/-}$ BrainSpheres. Compared with CHD8$^{+/+}$, *AUTS2* level was lower in NPCs but higher in BrainSpheres. We did not observe any statistically significant differences in expression of the autism risk genes *TC4*, *RELN,* and *PTEN* at any stage of neural differentiation. Thus, these results demonstrate similar efficiency of differentiation in both cell systems, with differences in expression of some autism and/or CHD8 targets [as previously reported by Wang et al. (2015, 2017)]. These results allowed further comparison of the response of both lines to treatment with CPF and CPO.

AChE Activity and ROS Levels in CHD8$^{+/+}$ *and CHD8*$^{+/-}$ *BrainSpheres*

We tested the sensitivity of both control and *CHD8*$^{+/-}$ BrainSpheres to CPF and its active metabolite, CPO. We treated

the spheroids at 4 and 8 wk of differentiation with 47 and 100 μM CPF or CPO, respectively, for 24 h. The treatment scheme is not a human relevant exposure scenario, but was rather used to model neurotoxic effects of the substances. Both concentrations were subtoxic, as measured by the resazurin reduction assay. *CHD8*$^{+/-}$ BrainSpheres, however, were slightly more sensitive to CPF and CPO at 8 wk (Figure 2A,B). For the next experiments, we selected 100 μM CPF and CPO concentrations and 4 wk of differentiation as an intermediate and immature stage of the differentiation process.

Previously, Slotkin and Seidler (2010) have shown that CPF induces oxidative stress in neuronal cultures. We analyzed the level of ROS and MMP. There were no significant differences in MMP aside from slightly lower levels of MMP upon treatment of CHD8$^{+/+}$ spheroids with CPO (Figure S3A). We observed higher levels of ROS in CHD8$^{+/-}$ than in CHD8$^{+/+}$ spheroids. No differences in ROS levels upon CPF/CPO treatment were found (Figure S3B), which may be attributed to assay limitations and the selected 24-h exposure.

Because AChE is the main target of CPF acutely, we quantified its enzymatic activity (Figure 2C). *AChE* gene expression was also assessed. As expected, CPO had a stronger inhibitory effect on AChE than CPF in both cell lines. Upon exposure to 100 μM CPF, AChE activity was lower by 41% and 37% in CHD8$^{+/+}$ and CHD8$^{+/-}$ BrainSpheres, respectively. Exposure to 100 μM CPO reduced AChE activity by 64% and 55% in CHD8$^{+/+}$ and CHD8$^{+/-}$ BrainSpheres, respectively. No significant difference was observed between the two cell lines. Interestingly, genetics affected *AChE* mRNA. CHD8$^{+/-}$ BrainSpheres had significantly lower levels of *AChE* mRNA (Figure 2D) when compared with CHD8$^{+/+}$ BrainSpheres. The level of AChE substrate—acetylcholine, measured intracellularly by MS—was higher after CPO treatment in both cell lines (Figure 2E). Based on two-way ANOVA analysis, genetics, exposure, and the interplay of both had

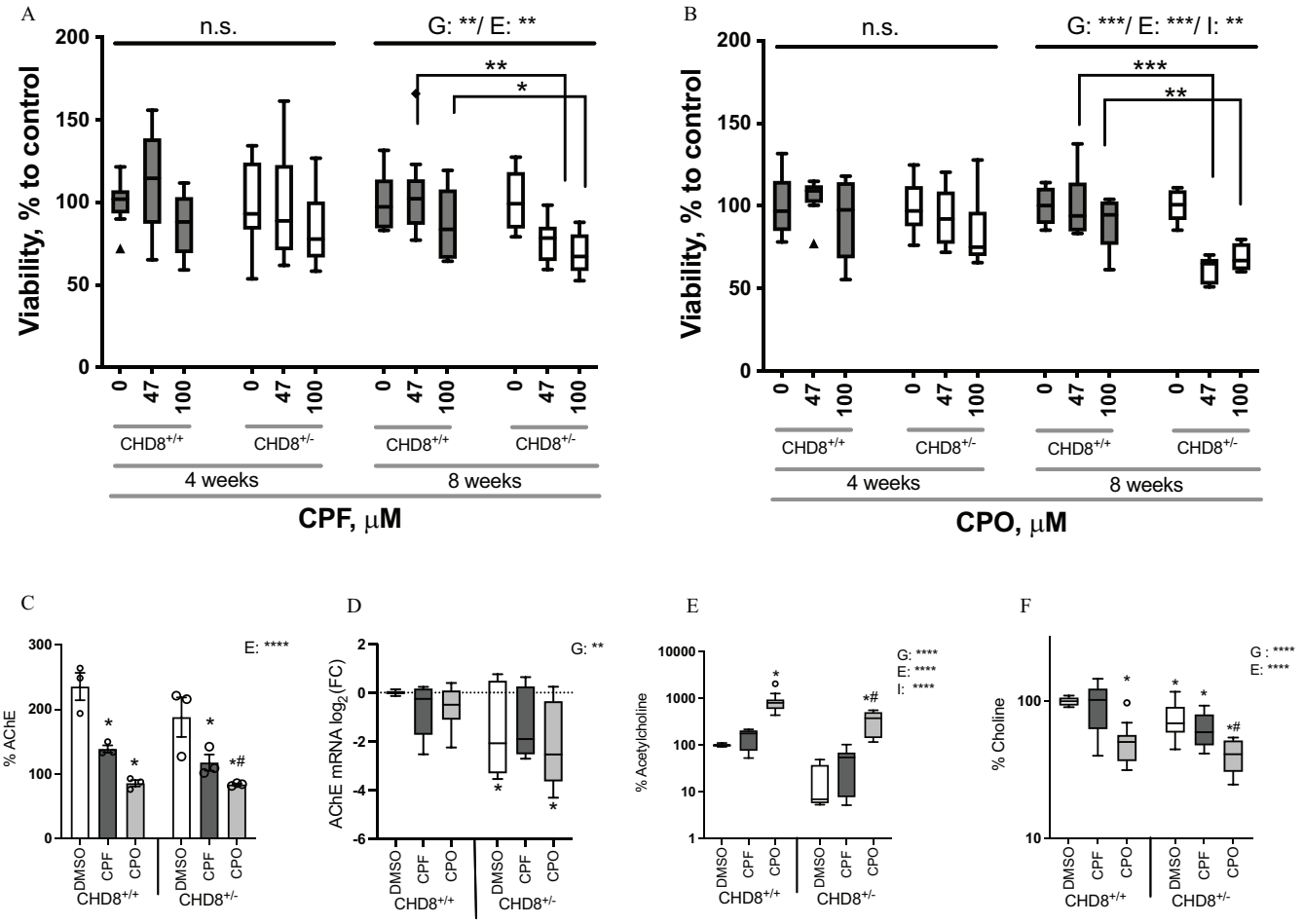

Figure 2. Cell viability and AChE activity after exposure to CPF or CPO. Resazurin reduction assay in 47 and 100 μM (A) CPF- and (B) CPO-treated *CHD8*$^{+/+}$ (gray) and *CHD8*$^{+/-}$ (white) BrainSpheres for 24 h at 4 and 8 wk of differentiation. The data represents three independent experiments with three technical replicates each (9 replicates in total, and 6 for 8-wk CPO treatment) normalized to DMSO vehicle-treated controls. Corresponding summary data are shown in Table S7. Asterisks after E, G, and I denote discovery of two-way ANOVA with posttest multiple comparisons for exposure effect between CHD8$^{+/+}$ and CHD8$^{+/-}$ BrainSpheres by the two-stage linear step-up procedure of Benjamini, Krieger, and Yekutieli and a desired false discovery rate (FDR) of 0.05. $^{*}p < 0.05$, $^{**}p < 0.01$, $^{***}p < 0.001$. (C) AChE activity: the data represent the AChE activity normalized to the protein amount in each sample (mean ± SEM, three independent experiments, $^{*}p < 0.01$, $^{****}p < 0.0001$); (D) mRNA expression (five independent experiments, with 7 technical replicates in total, $^{*}p < 0.05$, $^{**}p < 0.01$); intracellular levels of (E) acetylcholine and (F) choline measured at 4 wk of differentiation in *CHD8*$^{+/+}$ and *CHD8*$^{+/-}$ spheroids after exposure to 100 μM CPF (dark gray) and 100 μM CPO (light gray). DMSO vehicle-treated controls are depicted in white. Acetylcholine and choline were measured by LC-MS/MS in three independent experiments (12 technical replicates in total). Data were normalized to DMSO vehicle-treated *CHD8*$^{+/+}$ controls. Discovery of effect by genetics or by exposure or by (G × E) interaction on the metabolite levels was based on a two-way ANOVA with posttest multiple comparisons to **CHD8*$^{+/+}$ DMSO or $^{\#}$*CHD8*$^{+/-}$ DMSO by the two-stage linear step-up procedure of Benjamini, Krieger, and Yekutieli and a desired FDR of 0.01. $^{*}p < 0.01$, $^{****}p < 0.0001$. Corresponding summary data are shown in Tables S8 and S10. Note: AChE, acetylcholinesterase; ANOVA, analysis of variance; CPF, chlorpyrifos; CPO, oxon-metabolite of chlorpyrifos; DMSO, dimethyl sulfoxide; E, discovery of effect by exposure; G, discovery of effect by genetics; G × E, gene–environment; I, discovery of effects by G × E; n.s., not significant; SEM, standard error of the mean.

significant impacts on acetylcholine levels. The basal level of acetylcholine was higher in CHD8$^{+/+}$ than in CHD8$^{+/-}$ samples. Although the peak of acetylcholine in CHD8$^{+/+}$ BrainSpheres treated with CPO was higher than in CHD8$^{+/-}$, the magnitude of induction was greater in CHD8$^{+/-}$ BrainSpheres: an 18-fold vs. a 9-fold change difference in the CHD8$^{+/+}$ group of samples. We observed a slightly, but not significantly, higher level of acetylcholine in CPF-treated samples in both cell lines. This finding is supported by significantly lower AChE activity [possibly due to the presence of low levels of CPO in CPF-treated samples (Figure S4)], suggesting that BrainSpheres have the capacity to metabolize CPF to CPO. In accordance with these results, the level of choline was already lower by 26% in the mutant cell line than in the control, and was further reduced (59%) by CPO treatment (Figure 2F).

Neurite Outgrowth in CHD8$^{+/+}$ and CHD8$^{+/-}$ BrainSpheres Exposed to CPF or CPO

Because AChE is an essential factor regulating neurite outgrowth, we analyzed this process as a functional end point. BrainSpheres exposed to CPF/CPO had significantly shorter neurite length in both cell lines (Figure 3; Figures S5–S7). Pretreatment of spheroids with an antioxidant—tocopherol—attenuated the CPF effect. Although, in one of three experiments, there was a difference in neurite outgrowth between the untreated cell lines, the data was difficult to interpret owing to differences in spheroid size between the two cell lines. The magnitude of CPF and CPO effect was, however, similar in both cell lines, as indicated by AUC measurements (percentage differences are indicated in each figure; Figure 3; Figures S5–S7).

CHD8 mRNA and Protein Levels in CHD8$^{+/+}$ and CHD8$^{+/-}$ BrainSpheres Exposed to CPF or CPO

The next question addressed was whether CPF/CPO exposure could influence the level of CHD8 in BrainSpheres. In agreement with previous studies (Wang et al. 2017), we did not observe significant differences in *CHD8* mRNA expression between *CHD8*$^{+/+}$ and *CHD8*$^{+/-}$ BrainSpheres (Figure 4A). The expression pattern of *CHD8* reached its peak at 4 wk of differentiation and was reduced thereafter. CPF/CPO treatment did not significantly alter *CHD8* mRNA expression at 4 wk of differentiation (Figure 4B). We observed, however, significantly lower levels of CHD8 protein in BrainSpheres with the *CHD8* mutation (67% of *CHD8*$^{+/+}$), which were even lower (by 90%) after exposure (Figure 4C,D). CHD8$^{+/+}$ BrainSpheres treated with CPF had 80% lower CHD8 protein levels (Figure 4C).

Identification of ASD Metabolic Biomarkers from Literature

The key question was how to possibly validate *in vitro* data with clinical findings. We decided to use an exposomics approach (Sillé et al. 2020) in which population findings of biomarkers in biofluids are compared with differences in the mechanistic model (i.e.,

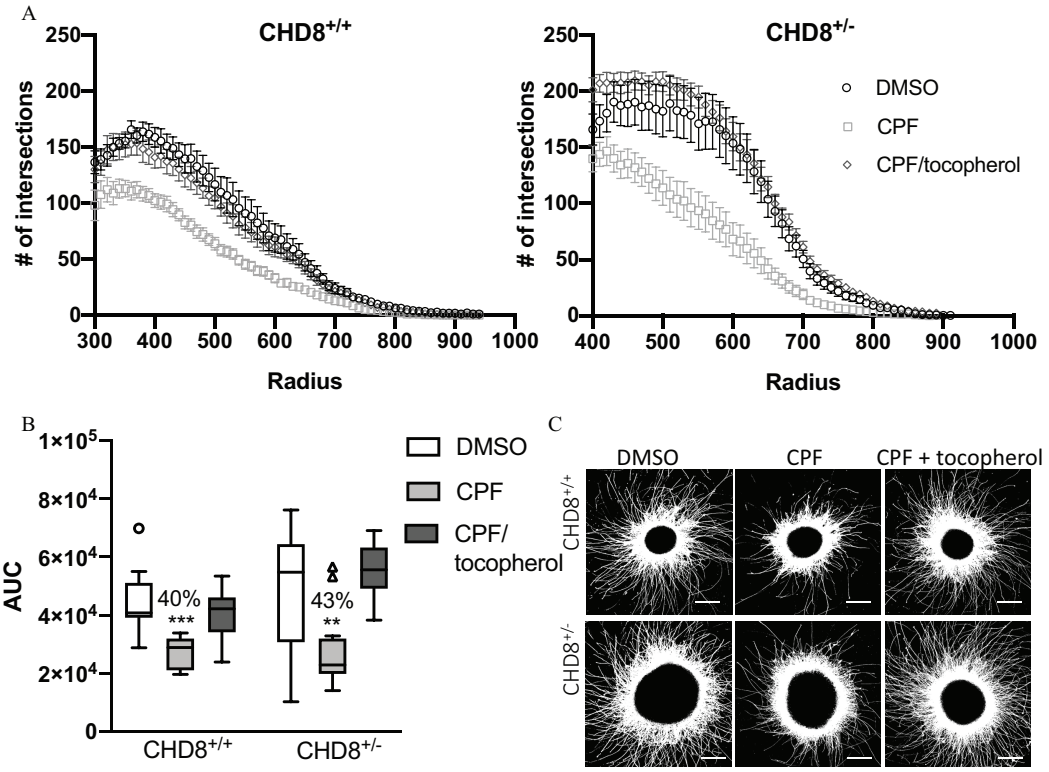

AUC	Control			CPF			CPF+ Vit. E		
	Mean	SD	N	Mean	SD	N	Mean	SD	N
CHD8+/+	45077	11433	10	27076	5549	12	40658	9125	8
CHD8+/-	49171	20246	11	27840	13262	13	54572	9436	12

Figure 3. Neurite outgrowth upon 100 μM CPF treatment and co-treatment with 100 μM tocopherol. (A) Sholl analysis of neurite outgrowth in *CHD8*$^{+/+}$ and *CHD8*$^{+/-}$ showing number of intersections (neurite density) starting from the edge of the spheroid. Each curve represents the mean ± SEM from 8 to 12 spheroids. (B) Area under the curve (AUC), calculated for each condition shown in (A). $^{**}p < 0.01$ and $^{***}p < 0.001$, one-way ANOVA with Holm-Sidak's posttest. (C) Representative images for each treatment. Scale bar: 200 μm. Note: ANOVA, analysis of variance; CPF, chlorpyrifos; DMSO, dimethyl sulfoxide; SD, standard deviation; SEM, standard error of the mean; Vit. E, tocopherol.

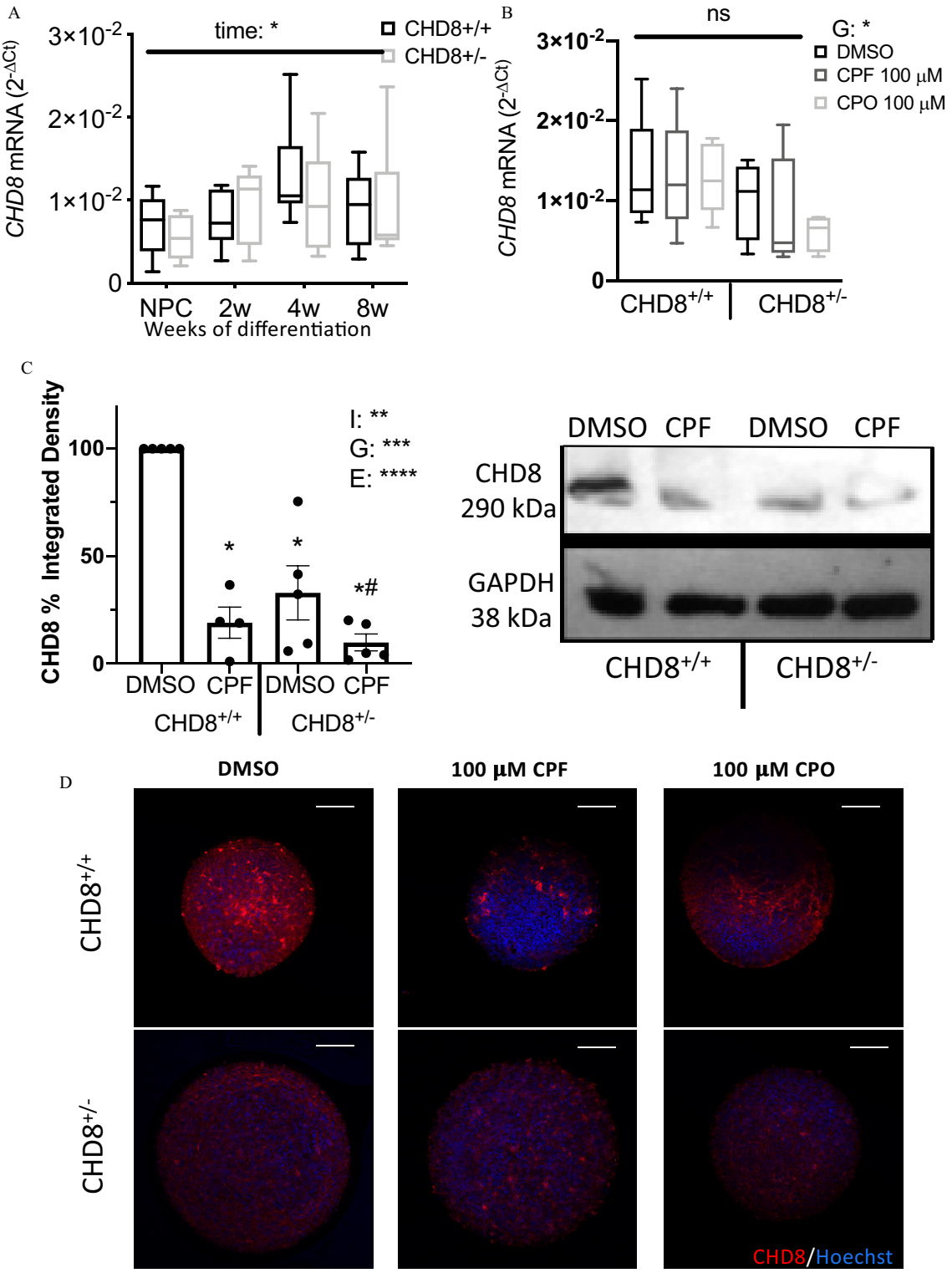

Figure 4. CHD8 expression upon CPF/CPO treatment. (A) *CHD8* gene expression in course of differentiation (four independent experiments). (B) *CHD8* gene expression in $CHD8^{+/+}$ and $CHD8^{+/-}$ BrainSpheres exposed to CPF/CPO (four independent experiments). (C) Western Blot quantification of CHD8 protein in $CHD8^{+/+}$ and $CHD8^{+/-}$ BrainSpheres treated with CPF. CHD8 protein level was normalized to GAPDH and is expressed as a percentage of $CHD8^{+/+}$ DMSO vehicle-treated control BrainSpheres. Dendrogram is shown as means ± SEMs (five independent experiments). Statistical significance was calculated by two-way ANOVA with posttest multiple comparisons to $^{*}CHD8^{+/+}$ DMSO or $^{\#}CHD8^{+/-}$ DMSO by the two-stage linear step-up procedure of Benjamini, Krieger, and Yekutieli and a desired false discovery rate of 0.05. $^{*}p < 0.05$, $^{**}p < 0.01$, $^{***}p < 0.001$, $^{****}p < 0.0001$. A representative blot is shown on the right side of (C). (D) Immunostaining of $CHD8^{+/+}$ and $CHD8^{+/-}$ BrainSpheres with CHD8 antibody (red) after CPF or CPO exposure. Representative images from three experiments are shown. Nuclei are stained with Hoechst 33342 (blue). Scale bar: 100 μm. Summary data (mean, SEM, N) are shown in Table S9. Note: ANOVA, analysis of variance; CPF, chlorpyrifos; CPO, oxon-metabolite of chlorpyrifos; DMSO, dimethyl sulfoxide; E, discovery of effect by exposure; G, discovery of effect by genetics; G × E, gene–environment; GADPH, glyceraldehyde-3-phosphate dehydrogenase; I, discovery of effect by (G × E) interaction; MS, mass spectrometry; NPC, neural progenitor cell; ns, not significant; SEM, standard error of the mean.

BrainSpheres). A comprehensive review of the literature identified a panel of pathways and metabolites perturbed in patients with ASD (e.g., amino acids, fatty acid metabolism, one-carbon metabolism, energy metabolism, oxidative stress, neurotransmitters). We selected a list of representative metabolites and neurotransmitters and compared the levels of those in the CPF/CPO-treated *CHD8*$^{+/+}$ and *CHD8*$^{+/-}$ BrainSpheres with human data (Table 1 and references therein). Notably, metabolite levels were sometimes contradictory, with some studies reporting higher and others lower levels in ASD vs. typically developed (TD) individuals. This might be due to the biological compartment for sampling, such as tissue or blood/urine or stage of the disease. We were therefore primarily interested in whether we could observe perturbations in these biomarkers as an indication of a perturbation of the linked pathways and not necessarily in the direction of the differences.

Effects of the CHD8 Mutation and CPF/CPO on Energy Metabolism, One-Carbon Metabolism, and Selected Neurotransmitters

We analyzed the intracellular levels of the 29 selected metabolites by MS and compared them between *CHD8*$^{+/+}$ and *CHD8*$^{+/-}$ BrainSpheres, with and without CPF and CPO treatment (Table S5). Twenty-three metabolites, which were significantly different ($p < 0.01$) in at least one condition, are shown in Table 1 and Table S10. We found perturbations in ASD metabolic biomarkers under either genetic alteration (14 metabolites), chemical treatment (17), or their combination (10).

Folate-dependent, one-carbon metabolism is a central hub in the cellular pathways and is essential for producing methyl groups for all methylation reactions. One-carbon metabolism plays a critical role in autism (James 2013; Orozco et al. 2019; Schaevitz and Berger-Sweeney 2012). SAM was affected by both genetics and exposure and its levels were higher in *CHD8*$^{+/-}$ BrainSpheres treated with CPF (+65%) and CPO (+134%) when compared with CHD8$^{+/+}$ DMSO samples. The basal level of SAH was 64% higher in *CHD8*$^{+/-}$ and further increased by CPF (+93%)- and CPO (+104%)-treated BrainSpheres, when compared with CHD8$^{+/+}$ DMSO samples. The SAM/SAH ratio was higher in CPO-treated samples in both cell lines (79% for CHD8$^{+/+}$ and 62% in CHD8$^{+/-}$) compared with corresponding DMSO-treated controls (Figure 5A). Although SAH levels were elevated in the urine and blood of patients with ASD, SAM levels were reduced (Table 1). Folic acid levels were higher in samples treated with CPF and CPO in both cell lines (Figure 5A); no effect of genetics was observed. No differences in methionine, reduced glutathione, and oxidized glutathione levels were detected. Cystathionine levels were significantly lower (−45%) only in *CHD8*$^{+/+}$ samples treated with CPO (Table 1).

Energy cycle (i.e., the citric acid cycle) metabolites were perturbed in patients with ASD (Orozco et al. 2019). In our experimental setup, creatine levels were slightly affected by the genetic factor, whereas lactic acid levels were found to be higher only in *CHD8*$^{+/-}$ BrainSpheres by 119% (CPF) and by 158% (CPO) when compared with DMSO-treated CHD8$^{+/+}$ BrainSpheres, and by 81% (CPF) and 113% (CPO) when compared with DMSO-treated CHD8$^{+/-}$ BrainSpheres. Similarly, L-tryptophan and its metabolite kynurenic acid (KA) had both significant genetic and exposure effects as assessed by two-way ANOVA, and their levels were elevated following CPF/CPO treatment only in the mutant cell line. Tryptophan levels were 58% higher in CPF- and 61% higher in CPO-treated *CHD8*$^{+/-}$ BrainSpheres, when compared with DMSO-treated *CHD8*$^{+/+}$ control BrainSpheres. When compared with DMSO-treated CHD8$^{+/-}$ BrainSpheres, levels were 43% and 46% higher for CPF and CPO, respectively. KA levels were higher after CPF and CPO treatment by 62% and 90%, respectively, when compared with DMSO-treated *CHD8*$^{+/+}$ control BrainSpheres (Figure 5C; Table 1). Levels of α-hydroxyglutaric acid were 433% higher in *CHD8*$^{+/-}$ spheres treated with CPO compared with DMSO-treated *CHD8*$^{+/+}$ control BrainSpheres, and 418% when compared with DMSO-treated *CHD8*$^{+/-}$ BrainSphere samples (Figure 5D).

Glutamate/GABA Ratio in CHD8$^{+/+}$ *and CHD8*$^{+/-}$ *BrainSpheres*

The imbalance of excitatory/inhibitory neuronal systems is known from population studies to be associated with ASD (reviewed by Gao and Penzes 2015). Consequently, we measured the levels of intracellular GABA and glutamate neurotransmitters. *CHD8*$^{+/-}$ BrainSpheres had 70% lower basal levels of GABA in comparison with *CHD8*$^{+/+}$ BrainSpheres, and a 255% higher ratio of glutamate vs. GABA (Figure 6). Exposure to CPF and CPO did not alter the glutamate/GABA ratio, but BrainSpheres treated with CPO had glutamate levels 67% and 75% higher in *CHD8*$^{+/+}$ and *CHD8*$^{+/-}$ BrainSpheres, respectively. Metabolites of arginine/ornithine/aspartate (urea) cycle were assessed. Arginine levels were significantly higher (+35%) in *CHD8*$^{+/+}$ BrainSpheres treated with CPF vs. corresponding controls. Although arginine had only exposure effects, both genetics and exposure affected ornithine—its levels were 55% lower in mutant BrainSpheres compared with *CHD8*$^{+/+}$ BrainSpheres and increased following CPF/CPO treatment by 66%/69% in the latter (Table 1). Higher ornithine and arginine levels were reported in the blood and urine in patients with ASD (Table 1).

CHD8 KO and CPF/CPO Effects on Dopaminergic System

We analyzed several parameters of the dopaminergic metabolism in our system. We observed no statistically significant differences in the levels of phenylalanine, exposure effects on tyrosine, higher levels of 1-3,4-dihydroxypyhenylalanine (levodopa; L-DOPA) due to the genetic factors, and 44% lower dopamine levels in *CHD8*$^{+/-}$ BrainSpheres with no differences due to treatment (Figure 7A). Gene expression of tyrosine hydroxylase (*TH*), an enzyme responsible for conversion of tyrosine to L-DOPA, was higher in BrainSpheres treated with CPF (Figure 7B). *COMT* (catechol-*O*-methyltransferase) expression was higher in *CHD8*$^{+/-}$ samples compared with *CHD8*$^{+/+}$ BrainSpheres (Figure 7B). Similarly, levels of SAM were also higher in the *CHD8*$^{+/-}$ group than in the control group (Figure 5A). Finally, we assessed the presence of TH^{+} dopaminergic neurons in the cultures and observed higher numbers of dopaminergic neurons in *CHD8*$^{+/-}$ and in *CHD8*$^{+/+}$ BrainSpheres exposed to CPO compared with *CHD8*$^{+/+}$ BrainSpheres (Figure 7C). Two different morphologies of the TH^{+} signal were observed: flat, nonneuronal-like cells were predominantly found in *CHD8*$^{+/+}$ BrainSpheres (marked with blue arrows in Figure 7C), and TH^{+} cells with distinctive neuronal morphology (marked with white arrowheads in Figure 7C) were predominantly found in *CHD8*$^{+/-}$ BrainSpheres.

Discussion

ASD is a genetically and phenotypically heterogeneous condition, making it difficult to identify factors that trigger the disease and influence the severity of symptoms. Although genetics has a substantial impact (Persico and Napolioni 2013), environmental factors also appear to play a role (Landrigan et al. 2012; Rylaarsdam and Guemez-Gamboa 2019; Sandin et al. 2014). Earlier studies showed that valproic acid, thalidomide, misoprostol, lead, and organophosphates contribute to ASD risk (Geier et al. 2009; Kuwagata et al. 2009; Landrigan 2010). We follow the hypothesis that exposures synergize with an individual's increased susceptibility, which would explain why genetic and environmental factors

Table 1. Metabolites, significantly ($p < 0.01$, 3 independent experiments) perturbed by *a*) *CHD8* mutation (genetic factor), *b*) CPF/CPO treatment (exposure factor), or *c*) *CHD8* mutation and CPF/CPO treatment (interaction) and existing knowledge on association of those metabolites with ASD.

	BrainSpheres			Literature					
				Brain		Blood		Urine	
Metabolite/KEGG ID	*CHD8*$^{+/-}$ (genetics)	CPF/CPO (exposure)	*CHD8*$^{+/-}$ CPF/CPO (interaction)	ASD vs. TD	References	ASD vs. TD	References	ASD vs. TD	References
L-Glutamic acid, C00025	—	Up	—	—	Kolodny et al. 2020; Cochran et al. 2015; Joshi et al. 2013	—	Orozco et al. 2019; Arnold et al. 2003; ElBaz et al. 2014	Down	Yap et al. 2010; Lussu et al. 2017; Evans et al. 2008, Nadal-Desbarats et al. 2014
				Up	Hassan et al. 2013; Brown et al. 2013; Joshi et al. 2013; Drenthen et al. 2016	Up	Tu et al. 2012; West et al. 2014; Aldred et al. 2003; Moreno-Fuenmayor et al. 1996; Shimmura et al. 2011; Tirouvanziam et al. 2012; Naushad et al. 2013; El-Ansary and Al-Ayadhi 2014; Cai et al. 2016; Shinohe et al. 2006; Hassan et al. 2013		
				Down	van Elst et al. 2014; Kubas et al. 2012; Horder et al. 2018	Down	El-Ansary 2016; Delaye et al. 2018		
GABA, C00025	Down	—	—	—	Kolodny et al. 2020; Harada et al. 2011; Brix et al. 2015; Horder et al. 2018	—	Saleem et al. 2020; ElBaz et al. 2014	Up	Cohen 2002
				Down	Cochran et al. 2015; Gaetz et al. 2014; Rojas et al. 2014; Kubas et al. 2012; Harada et al. 2011	Up	Dhossche et al. 2002; El-Ansary and Al-Ayadhi 2014		
L-Tyrosine, C00025	—	Up	Up[b]			—	Orozco et al. 2019; Saleem et al. 2020	Up	Gevi et al. 2016; Noto et al. 2014
						Up	Aldred et al. 2003	Down	Evans et al. 2008
						Down	Tu et al. 2012; Tirouvanziam et al. 2012; Naushad et al. 2013; ElBaz et al. 2014		
L-DOPA, C00355	Up	—	—						
Dopamine, C03758	Down	—	—	Down	Ernst et al. 1997	Up	Martineau et al. 1994; Hérault et al. 1993	Down	Martineau et al. 1994; Martineau et al. 1992
Choline, C00114	Down	Down	—	Down	Corrigan et al. 2013; Ford and Crewther 2016	—	Orozco et al. 2019		
Acetylcholine, C01996	Down	Up	Up[a,d]						
L-Tryptophan, C00078	Up	Up	Up[b,c]	—		—	Orozco et al. 2019	Up	Lussu et al. 2017
						Down	Tu et al. 2012; Saleem et al. 2020; Ormstad et al. 2018; Tirouvanziam et al. 2012; Bryn et al. 2017		
Kynurenic acid, C01717	Up	Up	Up[b,c,d]			Down	Ormstad et al. 2018; Bryn et al. 2017		
Kynurenine, C00328	—	Up	Up[b]					Down	Gevi et al. 2016
L-Alanine, C00041	—	Up	—			—	Saleem et al. 2020; Tirouvanziam et al. 2012; ElBaz et al. 2014	Up	Yap et al. 2010; Noto et al. 2014; Nadal-Desbarats et al. 2014
						Up	Orozco et al. 2019; Martineau et al. 1992; Aldred et al. 2003	Down	Ming et al. 2012; Hérault et al. 1993
D-Lactic acid, C00256						—	Orozco et al. 2019; Khemakhem et al. 2017	Down	Lussu et al. 2017
	Up	Up	Up[b,c]			Up	El-Ansary et al. 2017; Hassan et al. 2019		
						Down	West et al. 2014; Kuwabara et al. 2013		
Creatine, C00300	Down	—	—	Down	Ford and Crewther 2016			Up	Lussu et al. 2017
								Down	Bitar et al. 2018; Mavel et al. 2013

Table 1. (*Continued.*)

	BrainSpheres			Literature					
				Brain		Blood		Urine	
Metabolite/KEGG ID	*CHD8*$^{+/-}$ (genetics)	CPF/CPO (exposure)	*CHD8*$^{+/-}$ CPF/CPO (interaction)	ASD vs. TD	References	ASD vs. TD	References	ASD vs. TD	References
L-Arginine, C00062	—	Up	—			—	Orozco et al. 2019; Saleem et al. 2020; Tirouvanziam et al. 2012; ElBaz et al. 2014	Up	Liu et al. 2019
						Up	Kuwabara et al. 2013		
Ornithine, C01602	Down	Up	—			—	Saleem et al. 2020; ElBaz et al. 2014; Smith et al. 2019		
						Up	Orozco et al. 2019		
α-Hydroxyglutaric acid, C01087	—	Up	Up[b,c]					Up	Kałużna-Czaplińska et al. 2014
Folic acid, C00504	—	Up	—			—	Schaevitz and Berger-Sweeney 2012		
SAM, C00019	Up	Up	Up[b,c,d]			Down	James et al. 2004, 2006	Down	Geier et al. 2009
SAH, C00021	Up	—	Up[c,d]			Up	James et al. 2004, 2006	Up	Geier et al. 2009
L-Cysteine, C00097	Up	—	Up[c,d] ($p = 0.03$)[a]			—	Saleem et al. 2020	Down	Geier et al. 2009
						Down	Han et al. 2015; James et al. 2004, 2006; ElBaz et al. 2014		
Cystathionine, C02291		Down	Down ($p = 0.02$)[a,e]			Up	James et al. 2006	Down	Geier et al. 2009
						Down	James et al. 2004		
Cystine, C00491	—	Up	—			Up	Melnyk et al. 2012		
						Down	West et al. 2014		
N-Acetylaspartate, C01042	Down	Down		Down	Corrigan et al. 2013; Kubas et al. 2012; Ford and Crewther 2016				
Glutamate/GABA	Up		Down[b] ($p = 0.0109$)[a,e]						
SAM/SAH	Up	Up							
Cysteine/cystine	Up								

Note: *CHD8*$^{+/-}$ (genetics): significant changes in metabolites affected by genetics, based on a two-way ANOVA. CPF/CPO (exposure): metabolites, which were changed due to exposure, based on a two-way ANOVA. CHD8$^{+/-}$ and CPF/CPO (interaction). Data represents three independent experiments, with 12 technical replicates in total. If no direction is shown, it means no data were found. Summary data (mean, SD, SEM, N) are shown in Table S10. —, no difference to control was observed; ANOVA, analysis of variance; ASD, autism spectrum disorder; CPF, chlorpyrifos; CPO, oxon-metabolite of chlorpyrifos; DMSO, dimethyl sulfoxide; FDR, false discovery rate; GABA, gamma-aminobutyric acid; KEGG ID, Kyoto Encyclopedia of Genes and Genomes identifier; L-DOPA, 1-3,4-dihydroxypyhenylalanine or levodopa; SAH, *S*-adenosylhomocysteine; SAM, *S*-adenosylmethionine; SD, standard deviation; SEM, standard error of the mean; TD, typically developed.

[a]Interaction of both variables (genetics and exposure) identified by two-way ANOVA.

[b]Suggested interaction based on posttest multiple comparisons for exposures within the control and mutant groups by the two-stage linear step-up procedure of Benjamini, Krieger, and Yekutieli and a desired FDR of 0.01. Interaction was considered valid, if changes due to exposure were observed only in CHD8$^{+/-}$ but not in CHD8$^{+/+}$ BrainSpheres.

[c]Suggested interaction based on posttest multiple comparisons for exposures when comparing all conditions to CHD8$^{+/+}$ DMSO by the two-stage linear step-up procedure of Benjamini, Krieger, and Yekutieli and a desired FDR of 0.01. Interaction was considered valid, when metabolites, which were not different between *CHD8*$^{+/+}$ and *CHD8*$^{+/-}$ DMSO-treated samples, but were significantly altered due to CPF/CPO treatment in *CHD8*$^{+/-}$ BrainSpheres compared with control BrainSpheres (*CHD8*$^{+/+}$ DMSO) or the effects of *CHD8* mutation were enhanced with the treatment, when compared with *CHD8*$^{+/+}$ DMSO.

[d]Suggested interaction based on posttest multiple pairwise comparisons across the groups (DMSO$^{+/+}$ vs. DMSO$^{+/-}$, CPF$^{+/+}$ vs. CPF$^{+/-}$ and CPO$^{+/+}$ vs. CPO$^{+/-}$) by the two-stage linear step-up procedure of Benjamini, Krieger, and Yekutieli and a desired FDR of 0.01. Interaction was considered valid, when the significant changes were observed between treatment groups but not between DMSO controls. Up- or down-regulation vs. control are shown.

[e]FDR $p < 0.05$.

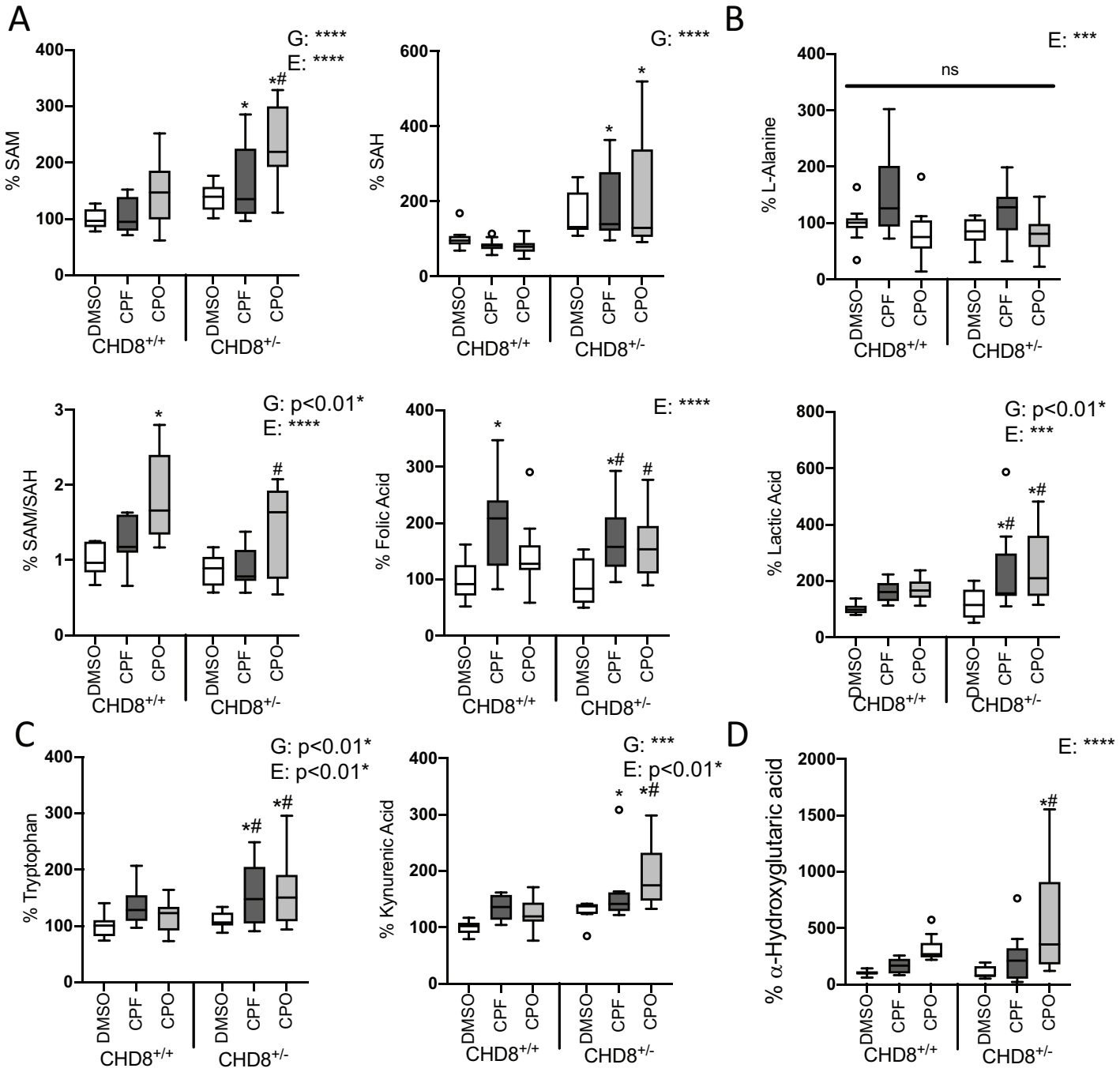

Figure 5. Effects of *CHD8* mutation and CPF/CPO exposure on key adverse outcome pathways of ASD. (A) Methyl donor system: SAM, SAH, SAM/SAH ratio, and folic acid. (B) L-alanine and lactic acid, (C) tryptophan and KA, and (D) α-hydroxyglutaric acid levels were measured by LC-MS/MS. DMSO vehicle-treated controls are depicted in white, CPF-treated in dark gray, and CPO in light gray. Data are normalized to DMSO vehicle-treated $CHD8^{+/+}$ control and represent results from three independent experiments (12 technical replicates in total, 8 for KA). Discovery of effect by genetics or by exposure was based on a two-way ANOVA with posttest multiple comparisons to $^{*}CHD8^{+/+}$ DMSO or $^{\#}CHD8^{+/-}$ DMSO by the two-stage linear step-up procedure of Benjamini, Krieger, and Yekutieli and a desired false discovery rate of 0.01. $^{*,\#}p<0.01$, $^{***}p<0.001$, $^{****}p<0.0001$. Summary data (mean, SD, SEM, N) are shown in Table S10. Note: ANOVA, analysis of variance; ASD, autism spectrum disorder; CPF, chlorpyrifos; CPO, oxon-metabolite of chlorpyrifos; DMSO, dimethyl sulfoxide; E, discovery of effect by exposure; G, discovery of effect by genetics; KA, kynurenic acid; LC, liquid chromatography; MS/MS, tandem mass spectrometry; SAM, *S*-adenosylmethionine; SAH, *S*-adenosylhomocysteine; SD, standard deviation; SEM, standard error of the mean.

are so difficult to identify in isolation. Accordingly, understanding of the mechanisms by which environment contributes is limited. One possibility is that environmental chemicals and susceptibility genes act on common targets. Assessing whether and how (G × E) interaction contributes to the etiology and severity of ASD could help rationalize prevention measures and drug development strategies. We suggest that a strong genetic background (e.g., mutation in a high-risk autism gene that alone can trigger the disease) can still synergize with environmental cofactors, thereby worsening symptoms and severity. Individuals with similar genetic variants can have significantly different symptoms and degrees of disease progression, including being on different levels of the ASD

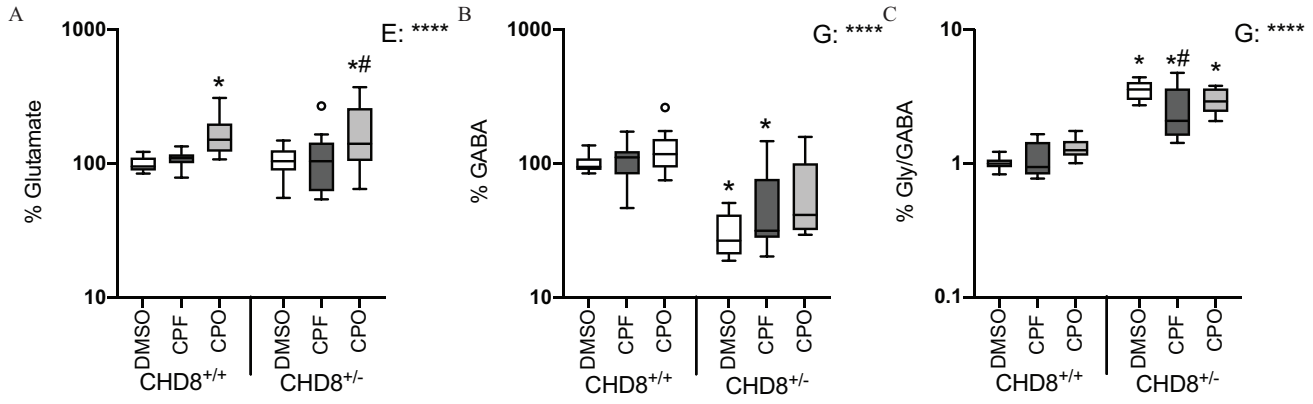

Figure 6. Excitatory/inhibitory neurotransmitters detection in *CHD8*$^{+/+}$ and *CHD8*$^{+/-}$ BrainSpheres after CPF/CPO exposure. (A) Glutamate and (B) GABA levels and (C) their ratio in *CHD8*$^{+/-}$ vs. *CHD8*$^{+/+}$ BrainSpheres treated with CPF (dark gray), CPO (light gray), or vehicle (white) were assessed by LC-MS/MS. Data from three independent experiments (12 technical replicates in total) normalized to DMSO vehicle-treated *CHD8*$^{+/+}$ controls is shown. Discovery of effect by genetics or by exposure was based on a two-way ANOVA with posttest multiple comparisons to **CHD8*$^{+/+}$ DMSO or $^{\#}$*CHD8*$^{+/-}$ DMSO by the two-stage linear step-up procedure of Benjamini, Krieger, and Yekutieli and a desired false discovery rate of 0.01. $^{*,\#}p<0.01$, $^{****}p<0.0001$. Summary data (mean, SD, SEM, N) are shown in Table S10. Note: ANOVA, analysis of variance; CPF, chlorpyrifos; CPO, oxon-metabolite of chlorpyrifos; DMSO, dimethyl sulfoxide; E, discovery of effect by exposure; G, discovery of effect by genetics; GABA, gamma-aminobutyric acid; Glu, Glutamate; Gly, glycine; LC, liquid chromatography; MS/MS, tandem mass spectrometry; SD, standard deviation; SEM, standard error of the mean.

spectrum, leaving substantial room for the contribution of environmental factors (Rylaarsdam and Guemez-Gamboa 2019). A cellular test with genetic susceptibility might be advantageous for identifying hazardous chemicals.

Approximately 65 high-autism-risk genes caused by *de novo* mutations were identified and can be clustered into two large groups: genes expressed early in development (during the first and second trimesters of pregnancy) and genes expressed later in pregnancy and after birth (Sanders 2015; Sanders et al. 2015). The first group includes transcription factors and chromatin remodelers, whereas the second group consists mainly of genes involved in synaptogenesis (Sanders 2015; Sanders et al. 2015). *CHD8*—a focus of this proof-of-principle study—belongs to the first group and is one of the nine high-confidence autism genes (Willsey et al. 2013) that can also regulate the expression of other autism-related genes (Cotney et al. 2015). It is therefore an attractive candidate for synergies with exposures at early embryonic stages as reflected in the BrainSphere model. Notably, the model without genetic alteration was sensitive to the pesticide rotenone (Pamies et al. 2018) and the drug paroxetine (Zhong et al. 2020), demonstrating its utility as a developmental toxicity model. The model is also supported by the U.S. Environmental Protection Agency for developing an animal-free method for this purpose (Wheeler 2019).

Traditional validation of the findings with animal studies is not only cost prohibitive [at $1.4 million per chemical (Smirnova et al. 2014)], but animal findings on the effects of CPF are also controversial (Mie et al. 2018). The rat is the standard species used for neurotoxicity and developmental neurotoxicity tests [according to Organisation for Economic Co-operation and Development test guidelines 424 (OECD 1997), 426 (OECD 2007), and 443 (OECD 2018)]. *Chd8* KO rats are not available, and although there is a *Chd8 KO* mouse model (Platt et al. 2017; Suetterlin et al. 2018) that shows ASD features, the mouse is not a standard model organism for neurotoxicity testing. Although autism is unique for humans, animal models can provide some insight into the behavioral biology, whereas complex *in vitro* models—as used here—allow mechanistic studies with the focus on biomarkers and molecular signatures. (G × E) interaction analyses focusing on neurotoxicity and carried out using brain organotypic cultures specifically will provide more complex cellular architecture and interactions than traditional monolayer cultures. In addition, using human brain models provides an opportunity to compare *in vitro* findings with clinical data from patients. Finally, the established AOPs for developmental neurotoxicity (Bal-Price et al. 2015, 2017; Li et al. 2019) allow us to focus on specific key events associated with neurotoxicity and developmental neurotoxicity AOPs. The current *in vitro* models, however, including the one described here, still have some limitations, including, for example, the lack of interorgan communication, the absence of hormonal factors and the immune system, limited metabolism, and inability to predict behavioral outcomes. The combination of *in vitro*, *in vivo*, nonmammalian models, and human clinical data are most promising (Halladay et al. 2009) until the *in vitro* approach is mature enough to replace the animal and translate to the human situation.

A key use of our model is for regulatory testing of chemicals for possible effects on neurodevelopment by using a cell system susceptible to developmental neurotoxicants. This regulatory use requires formal validation (Hartung et al. 2004; Leist et al. 2012) of the model. However, an insufficient number of chemicals have been tested in the respective animal guideline tests. We suggested earlier mechanistic validation of a model (Hartung et al. 2013), that is, by demonstrating that relevant mechanisms are reflected instead of the mere correlation with findings from animal studies. This would ideally be done on the basis of an agreed AOP, but, in this case, the AOP of DNTs have not been sufficiently developed and accepted. Nevertheless, there is a substantial body of clinical and epidemiological findings on autism pathophysiology, metabolic biomarkers, and associations with the environment. These lend themselves to validation by correlation with findings obtained with the model system. This was suggested as a human exposome approach (Sillé et al. 2020).

Here, we attempted to correlate the metabolic perturbations observed in our human brain model carrying a high-risk autism mutation in the *CHD8* gene, exposed to a model environmental toxicant—CPF—with findings in epidemiological and clinical studies. We established a synergy between the risk gene and the risk exposure. Our results demonstrate that, based on the resazurin assay, *CHD8*$^{+/-}$ was slightly more sensitive to CPO insult in general. A key finding of our study was that *CHD8*$^{+/-}$ cells exposed to CPF had lower levels of the CHD8 protein compared with those exposed to the control condition, showing potential synergy of CPF and CPO with the *CHD8* mutation and possible

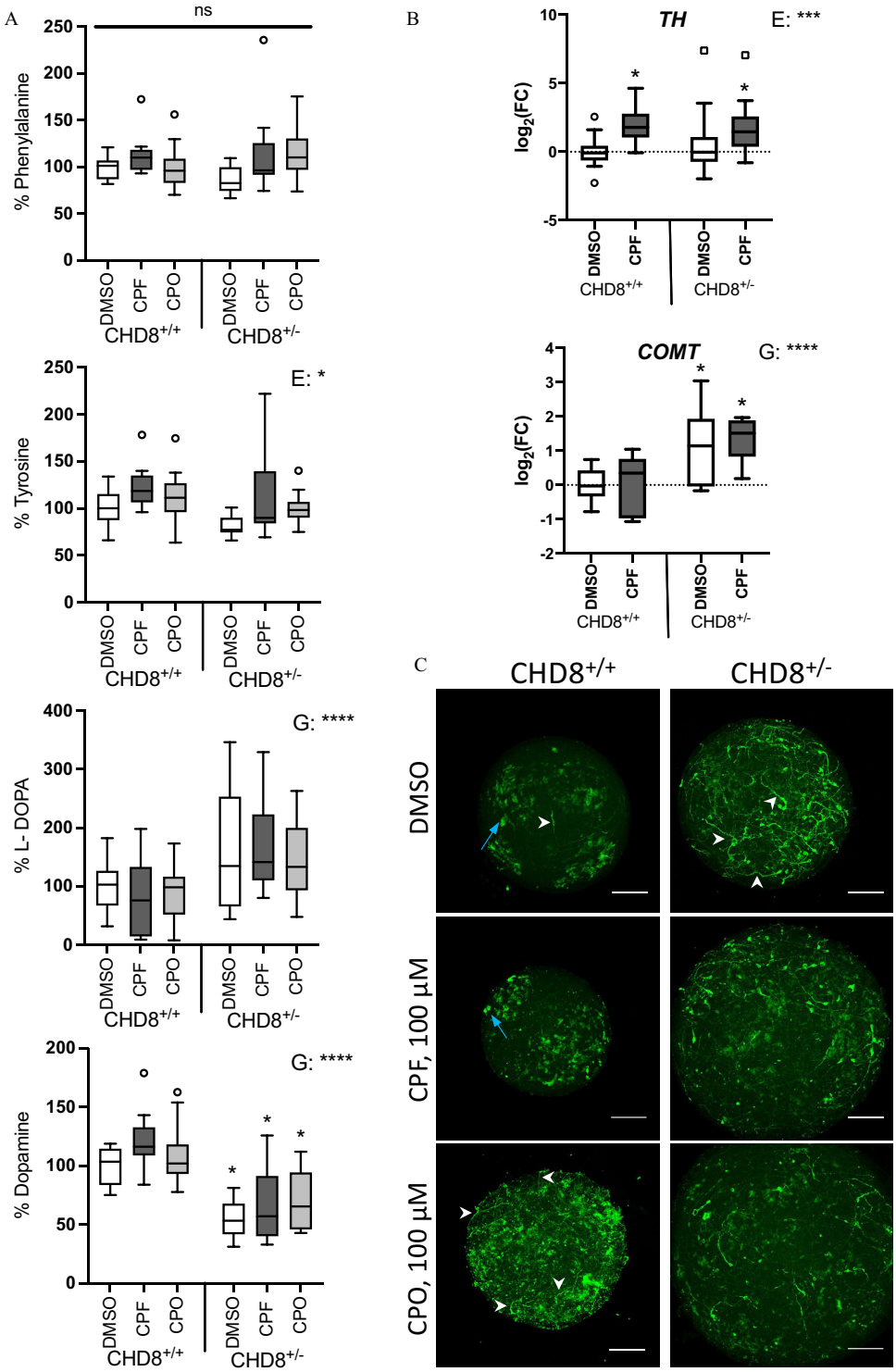

Figure 7. Perturbations of the dopaminergic system in $CHD8^{+/+}$ vs. $CHD8^{+/-}$ BrainSpheres after CPF/CPO treatment. (A) Levels of phenylalanine, tyrosine, L-DOPA, and dopamine were measured by LC-MS/MS. Data from three independent experiments (12 technical replicates in total) normalized to DMSO vehicle-treated $CHD8^{+/+}$ controls is shown. Discovery of effect by genetics or by exposure was based on a two-way ANOVA with posttest multiple comparisons to *CHD8*$^{+/+}$ DMSO by the two-stage linear step-up procedure of Benjamini, Krieger, and Yekutieli and a desired false discovery rate (FDR) of 0.01. $^{*}p < 0.01$, $^{****}p < 0.0001$. (B) RT-PCR of tyrosine hydroxylase (TH) and catechol-*O*-methyltransferase (COMT) in both cell lines treated with CPF. Data represent $\log_2(2^{-\Delta\Delta Ct})$ of at least three independent experiments with 11 to 16 technical replicates in total. Discovery of effect by genetics or by exposure was based on a two-way ANOVA with posttest multiple comparisons to *CHD8*$^{+/+}$ DMSO by the two-stage linear step-up procedure of Benjamini, Krieger, and Yekutieli and a desired FDR of 0.05. $^{*}p < 0.05$, $^{***}p < 0.001$, $^{****}p < 0.0001$. (C) Immunohistochemistry with anti-TH–specific antibody (green) of $CHD8^{+/+}$ and $CHD8^{+/-}$ BrainSpheres treated with CPF/CPO. White arrowheads indicate neuronal-shaped cells, blue arrows indicate flat clusters of cells. Nuclei were stained with Hoechst 33342 (blue). Scale bar: 100 µm. Summary data (mean, SD, SEM, N) are shown in Tables S9 and S10. Note: ANOVA, analysis of variance; CPF, chlorpyrifos; CPO, oxon-metabolite of chlorpyrifos; DMSO, dimethyl sulfoxide; E, discovery of effect by exposure; G, discovery of effect by genetics; LC, liquid chromatography; L-DOPA, 1-3,4-dihydroxypyhenylalanine (or levodopa); MS/MS, tandem mass spectroscopy; ns, not significant; RT-PCR, real-time polymerase chain reaction; SD, standard deviation; SEM, standard error of the mean.

further interactions on downstream targets that may be crucial for neural development and disease progression. In addition, the fact that lower levels of CHD8 were observed at the protein level, but not at the mRNA level, suggests a posttranscriptional interaction. However, further research is needed to address the effects of CPF and CPO on CHD8 molecular networks during development.

Further potential synergy between the CHD8 mutation and CPF/CPO exposure emerged from our metabolomics analysis where we were able to demonstrate the potential of comparing *in vitro* findings with human clinical data. Alterations of some metabolites associated with ASD were also affected by the combination of the *CHD8* mutation and CPF and/or CPO treatment.

Dysfunction of cholinergic activity in individuals with ASD has been linked to social and behavioral abnormalities, including sensory processing and attention reorienting behavior (Ford and Crewther 2016; Orekhova and Stroganova 2014). The supposed primary acute mode of action of OPs is via AChE—the main target of CPO. Choline levels were lower in patients with ASD (Table 1), as mirrored by the *CHD8* mutation in our model. Synergistically, CPO exposure led to a greater accumulation of acetylcholine in CHD8$^{+/-}$ BrainSpheres—demonstrating an increased susceptibility of mutant BrainSpheres to CPF/CPO toxic effects with respect to cholinergic dysfunction (Figure 2C–F).

Folate-dependent, one-carbon metabolism, and transsulfuration pathways can be perturbed in ASD (Orozco et al. 2019), showing alterations of methyl donor SAM in patients with ASD. Although lower levels of SAM and higher levels of SAH were reported in the biofluids of patients with ASD (Table 1), in our system, we detected elevated levels of both SAM and SAH only in mutant BrainSpheres, suggesting additive effects of genetics and exposure (Figure 5A). Higher expression of the methyltransferase *COMT* (Figure 7B) and elevated SAM would suggest hypermethylation in *CHD8*$^{+/-}$ BrainSpheres, but in this case, lower SAH levels would be expected—which is not what we observed. More detailed analyses are required to clarify mechanisms, but the findings indicate a perturbation of this pathway by both mutation and exposure.

Elevated plasma alanine and lactate in patients with ASD suggest peripheral mitochondrial dysfunction associated with this disorder (Aldred et al. 2003; El-Ansary et al. 2017; Orozco et al. 2019). Although we were not able to see any significant differences in MMP in our system, lactic acid levels were higher after treatment with both CPF and CPO in *CHD8*$^{+/-}$ BrainSpheres only (Figure 5B)—an indication of additive effects from exposure and genetics.

Plasma levels of tryptophan and its metabolite KA were reported to be attenuated in ASD (Table 1), whereas higher brain levels of KA were found in animal models of ASD and attention deficit hyperactivity disorder (Murakami et al. 2019; McTighe SM et al. 2013) and in the postmortem brains of patients with schizophrenia (Iaccarino et al. 2013). This was associated with the cognitive, behavioral, and learning impairments characterizing these disorders (Iaccarino et al. 2013; Murakami et al. 2019; Scharfman et al. 2000; Vohra et al. 2018; Yerys et al. 2009). In agreement with those findings, we found higher levels of tryptophan and KA in our *CHD8*$^{+/-}$ BrainSpheres exposed to CPF/CPO (Figure 5C). Tryptophan is known as the precursor of serotonin, but it was suggested that the great majority of tryptophan enters the kynurenine pathway, leading to the production of several neuroactive compounds, including KA (Kałużna-Czaplińska et al. 2017). KA can interact with *N*-methyl-D-aspartate, nicotinic, and G-protein coupled receptor 35 receptors, affecting cognition, neural plasticity, and brain development through the modulation of glutamate, dopamine, acetylcholine, and GABA release (Iaccarino et al. 2013; Kałużna-Czaplińska et al. 2017). Furthermore, KA functions as a ROS scavenger, thereby playing a role in redox homeostasis (Ramos-Chávez et al. 2018). A higher level of oxidative stress is a known feature of ASD (Chauhan and Chauhan 2006). Thus, compensatory elevated KA may be a result of the higher oxidative stress observed in *CHD8*$^{+/-}$ BrainSpheres (Figure S3B).

The physiological functions of α-hydroxyglutaric acid remain widely unknown, but its accumulation was found to be toxic to the mammalian brain (van Schaftingen et al. 2009). α-Hydroxyglutaric aciduria in the urine, plasma, and cerebrospinal fluid were associated with diverse neurologic deficits (Zafeiriou et al. 2008). Interestingly, α-hydroxyglutaric aciduria was observed in a few ASD case reports (Zafeiriou et al. 2008; Kiykim E et al. 2016). Furthermore, α-hydroxyglutaric acid has been shown to inhibit mitochondrial creatine kinase and to induce oxidative stress in the cerebellum (van Schaftingen et al. 2009). Our metabolomic analysis revealed higher levels of α-hydroxyglutaric acid in *CHD8*$^{+/-}$ BrainSpheres exposed to CPO when compared with both *CHD8*$^{+/+}$ and *CHD8*$^{+/-}$ DMSO-treated controls (Figure 5D), suggesting that the *CHD8* mutant BrainSpheres are more sensitive to CPO and the higher 2-hydroxyglutaric acid levels might be due to the synergistic effect of the *CHD8* mutation and exposure to CPO. It is difficult, however, to speculate about the mechanism behind this finding. Further analysis is needed to distinguish between α and β forms.

We also observed one of the main ASD features: an imbalance in excitatory and inhibitory neurotransmitters in *CHD8*$^{+/-}$ BrainSpheres (Figure 6). About 80% of the neurons in the cerebral cortex are excitatory, and the remaining 20% are inhibitory (represented primarily by GABAergic interneurons). In some studies, lower levels of GABA and numbers of GABAergic interneurons were found in mouse models of ASD (Gogolla et al. 2009; Rippon et al. 2007; Rubenstein and Merzenich 2003), which was also consistent with a higher incidence of epilepsy in humans with ASD (Lewine et al. 1999) and in ASD mouse models (Belmonte et al. 2004; Rubenstein and Merzenich 2003). The lower level of GABA neurotransmission in sound processing and motor control regions may be the cause of hypersensitivity of autistic patients to loud sounds and motor impairment (Gaetz et al. 2014). In other studies involving iPSCs (Mariani et al. 2015) and postmortem samples of five individuals with autism and five without (Lawrence et al. 2010), a higher number of GABAergic interneurons was associated with the ASD phenotype. This discrepancy may be due to the genetic heterogeneity of autistic patients, changes occurring during the life span, or different brain regions analyzed in reported studies. In our system, the *CHD8* heterozygous KO condition resulted in lower levels of GABA, which were not significantly altered with CPF/CPO treatment. Interestingly, expression of the GABAergic transcription factor *DLX1,* which regulates glutamic acid decarboxylase 1 (*GAD1)* expression (among many other genes), was higher in *CHD8*$^{+/-}$ BrainSpheres, such that an elevated level of GABA might be expected. But neither GAD1 nor GABA levels were higher. Here, more experiments are needed to understand and validate the exact mechanism of this circuit. Excessive and unbalanced excitatory glutamatergic signaling was associated with the high epilepsy rates in ASD (Zheng et al. 2016). Glutamate levels were significantly higher in both *CHD8*$^{+/+}$ and *CHD8*$^{+/-}$ BrainSpheres exposed to CPO. In a recent meta-analysis, Zheng et al. (2016) established overall higher blood glutamate levels in ASD than in typically developing individuals, with a positive correlation between glutamate levels in ASD blood and brain samples. Thus, further investigations are needed to elucidate whether CPO is specifically correlated with an increased risk of developing forms of ASD associated with epilepsy, which is present in about 20% of patients with ASD (Besag 2017). Abnormalities in the arginine/ornithine/aspartate (urea) cycle in patients with ASD has also been reported (Liu et al. 2019). Given that glutamate and ornithine

are linked, alterations in the urea cycle can play a role in the excitatory/inhibitory imbalance.

CPF has been found to affect dopaminergic neurons *in vivo* (Aldridge et al. 2005; Torres-Altoro et al. 2011; Zhang et al. 2015). Imbalanced levels of dopamine have been reported in ASD (Pavăl 2017; Marotta et al. 2020), but the observations were not consistent. The dopamine synthesis pathway was perturbed in our experimental model system by both exposure to CPF/CPO and CHD8 mutation (Figure 7). Interestingly, we observed slightly higher levels of L-DOPA along with lower level of dopamine in *CHD8*$^{+/-}$ BrainSpheres, but no changes due to CPF/CPO treatment. Moreover, *TH* expression was higher due to exposure, whereas *COMT* expression was higher due to genetics. Although there is some controversy in the literature reporting both higher and lower levels of dopamine in ASD vs. TD individuals, the perturbation of catecholamine synthesis in ASD has been established (Ernst et al. 1997; Kałużna-Czaplińska et al. 2010). *COMT* gene variations have been associated with ASD, anxiety, and bipolar disorders (James et al. 2006; Lachman 2008; Lachman et al. 1996; Schmidt et al. 2011). Elevated COMT activity due to functional polymorphism (Val158) has been associated with lower levels of dopamine, poorer cognitive performance, and greater predisposition for psychiatric disorders (Kamath et al. 2012; Simpson et al. 2014). Given that COMT initiates catecholamine degradation by transferring a methyl group from SAM to catecholamines, the higher expression of *COMT* and lower levels of dopamine, in our analysis, suggests that dopamine is metabolized more rapidly in *CHD8*$^{+/-}$ BrainSpheres.

Overall, our targeted metabolomics findings are consistent with a dysregulation in glutamate, GABA, catecholamines, and acetylcholine neurotransmitter systems, as previously reported in ASD and summarized by Cetin et al. (2015) and Marotta et al. (2020). Here, we recapitulated some of the key findings from the literature and demonstrated the potential contribution of a (G × E) interaction to an imbalance in neurotransmission. Although the changes in biofluids and in our model, as well as in the aforementioned animal models, were sometimes contradictory (such as those in tryptophan and SAM/SAH), we interpret them as perturbations in the same pathway. Alternatively, the differences could be due to analysis of intracellular metabolites *in vitro*, whereas the clinical findings are mainly in blood and urine. Additional quantification of these metabolites and neurotransmitters in the medium supernatant to model clinical biofluid findings could contribute to a better understanding of the perturbation of these pathways.

As a direct outcome of perturbations in energy metabolism and acetylcholine degradation, the highly energy-dependent process of neurite outgrowth was assessed (Figure 3; Figure S7). As expected, both CPF and CPO significantly impaired neurite outgrowth. This effect could be rescued by pretreatment with tocopherol, confirming perturbation in energy metabolism and oxidative stress. We have not directly observed higher ROS levels in response to CPF or CPO exposure (Figure S3B), likely due to the 24-h exposure selected. Because of the different spheroid sizes, we were unable to draw a conclusion about synergistic effects on neurite outgrowth between exposure and *CHD8* mutation, but based on our data the magnitude of the alterations were similar in the two cell lines. Axonal growth was shown to be perturbed by OPs in the developing nervous system. In neural cell lines, CPF has been shown to inhibit neurite outgrowth, whereas axonal growth has been shown to be perturbed by CPF in rat primary neurons (Howard et al. 2005; Yang et al. 2008). Taken together, the data indicate that *CHD8*$^{+/-}$ and CPF/CPO can both impair neurodevelopment, given that increased ROS production and impaired neurite outgrowth are key events of the DNT AOP.

In conclusion, this study demonstrated how an iPSC-derived 3D brain model can be used in studying a known genetic ASD risk factor and the exposure to an environmental chemical and to address whether and how these two factors can synergize. Remarkably, common metabolic targets for both the *CHD8* mutation and CPF/CPO exposure suggest that CPF can mimic some effects of *CHD8*$^{+/-}$ and vice versa, especially because cells treated with CPF had lower CHD8 protein levels than those treated with vehicle. This suggests that in patients with *CHD8* mutations, severity of symptoms might be exacerbated if they are exposed to this toxicant. Although only two cell lines were used in this study (control and selectively mutated), the findings point to potential targets and adverse outcomes to evaluate when performing (G × E) interaction studies. Extension of these findings to more human-relevant exposure scenarios, different developmental neurotoxicants, and more cell lines (including patient-derived iPSCs), is needed to validate the findings presented here. The identification of defined (G × E) interaction factors converging on common metabolic pathways could then foster the development of treatments tailored to specific clusters of patients.

These types of (G × E) interaction in organotypic models (Marx et al. 2016, 2020) represent a way forward to study the interplay of genetic and environmental components of autism and other neurodevelopmental disorders. The mechanistic validation through consensus AOP, and especially the corroboration with biomarker identification and correlation between clinical and mechanistic studies, opens new approaches for establishing the relevance of such findings.

Acknowledgments

S.M. and X.Z. conducted experiments and performed data analysis, S.M. contributed to manuscript preparation, Y.M. and A.K. conducted mass spectrometry analysis, F.F. supported experiments on neurite outgrowth and mass spectrometry, D.P. supported BrainSphere differentiation, H.T.H. and V.C. supported experimental design, H.L. generated the cell lines and differentiated induced pluripotent stem cells to neural progenitor cells, T.H. contributed to manuscript preparation, L.S. supervised the research of S.M., X.Z., and F.F., designed the experiments, conducted the data analysis/integration, and prepared the manuscript. We thank D. Costa for the graphical abstract design. We acknowledge Bloomberg Flow Cytometry and Immunology core and, in particular, T. Nilles.

Metabolomics and gene expression elements of this study were supported by the Alternatives Research and Development Foundation as an Air Challenge grant. The study was supported by a U.S. Environmental Protection Agency Science to Achieve Results program grant (R839505). X.Z. was supported by a grant from the China Scholarship Council (201506370074).

References

Aldred S, Moore KM, Fitzgerald M, Waring RH. 2003. Plasma amino acid levels in children with autism and their families. J Autism Dev Disord 33(1):93–97, PMID: 12708584, https://doi.org/10.1023/A:1022238706604.

Aldridge JE, Meyer A, Seidler FJ, Slotkin TA. 2005. Alterations in central nervous system serotonergic and dopaminergic synaptic activity in adulthood after prenatal or neonatal chlorpyrifos exposure. Environ Health Perspect 113(8):1027–1031, PMID: 16079074, https://doi.org/10.1289/ehp.7968.

Arnold GL, Hyman SL, Mooney RA, Kirby RS. 2003. Plasma amino acids profiles in children with autism: potential risk of nutritional deficiencies. J Autism Dev Disord 33(4):449–454, PMID: 12959424, https://doi.org/10.1023/a:1025071014191.

Astashkina A, Grainger DW. 2014. Critical analysis of 3-D organoid in vitro cell culture models for high-throughput drug candidate toxicity assessments. Adv Drug Deliv Rev 69–70:1–18, PMID: 24613390, https://doi.org/10.1016/j.addr.2014.02.008.

Ayhan F, Konopka G. 2019. Regulatory genes and pathways disrupted in autism spectrum disorders. Prog Neuropsychopharmacol Biol Psychiatry 89:57–64, PMID: 30165121, https://doi.org/10.1016/j.pnpbp.2018.08.017.

Bal-Price A, Crofton KM, Leist M, Allen S, Arand M, Buetler T, et al. 2015. International STakeholder NETwork (ISTNET): creating a developmental neurotoxicity (DNT) testing road map for regulatory purposes. Arch Toxicol 89(2):269–287, PMID: 25618548, https://doi.org/10.1007/s00204-015-1464-2.

Bal-Price A, Lein PJ, Keil KP, Sethi S, Shafer T, Barenys M, et al. 2017. Developing and applying the adverse outcome pathway concept for understanding and predicting neurotoxicity. Neurotoxicology 59:240–255, PMID: 27212452, https://doi.org/10.1016/j.neuro.2016.05.010.

Baxter AJ, Brugha TS, Erskine HE, Scheurer RW, Vos T, Scott JG. 2015. The epidemiology and global burden of autism spectrum disorders. Psychol Med 45(3):601–613, PMID: 25108395, https://doi.org/10.1017/S003329171400172X.

Beger RD, Dunn WB, Bandukwala A, Bethan B, Broadhurst D, Clish CB, et al. 2019. Towards quality assurance and quality control in untargeted metabolomics studies. Metabolomics 15(1):4, PMID: 30830465, https://doi.org/10.1007/s11306-018-1460-7.

Belmonte MK, Cook EH Jr, Anderson GM, Rubenstein JLR, Greenough WT, Beckel-Mitchener A, et al. 2004. Autism as a disorder of neural information processing: directions for research and targets for therapy. Mol Psychiatry 9(7):646–663, PMID: 15037868, https://doi.org/10.1038/sj.mp.4001499.

Benjamini Y, Krieger AM, Yekutieli D. 2006. Adaptive linear step-up procedures that control the false discovery rate. Biometrika 93(3):491–507, https://doi.org/10.1093/biomet/93.3.491.

Bernier R, Golzio C, Xiong B, Stessman HA, Coe BP, Penn O, et al. 2014. Disruptive *CHD8* mutations define a subtype of autism early in development. Cell 158(2):263–276, PMID: 24998929, https://doi.org/10.1016/j.cell.2014.06.017.

Besag FM. 2017. Epilepsy in patients with autism: links, risks and treatment challenges. Neuropsychiatr Dis Treat 14:1–10, PMID: 29296085, https://doi.org/10.2147/NDT.S120509.

Bitar T, Mavel S, Emond P, Nadal-Desbarats L, Lefèvre A, Mattar H, et al. 2018. Identification of metabolic pathway disturbances using multimodal metabolomics in autistic disorders in a Middle Eastern population. J Pharm Biomed Anal 152:57–65, PMID: 29414019, https://doi.org/10.1016/j.jpba.2018.01.007.

Bouhifd M, Beger R, Flynn T, Guo L, Harris G, Hogberg H, et al. 2015. Quality assurance of metabolomics. ALTEX 32(4):319–326, PMID: 26536290, https://doi.org/10.14573/altex.1509161.

Brännvall K, Bergman K, Wallenquist U, Svahn S, Bowden T, Hilborn J, et al. 2007. Enhanced neuronal differentiation in a three-dimensional collagen-hyaluronan matrix. J Neurosci Res 85(10):2138–2146, PMID: 17520747, https://doi.org/10.1002/jnr.21358.

Brix MK, Ersland L, Hugdahl K, Grüner R, Posserud M-B, Hammar Å, et al. 2015. Brain MR spectroscopy in autism spectrum disorder—the GABA excitatory/inhibitory imbalance theory revisited. Front Hum Neurosci 9:365, PMID: 26157380, https://doi.org/10.3389/fnhum.2015.00365.

Brown MS, Singel D, Hepburn S, Rojas DC. 2013. Increased glutamate concentration in the auditory cortex of persons with autism and first-degree relatives: a ^{1}H-MRS study. Autism Res 6(1):1–10, PMID: 23166003, https://doi.org/10.1002/aur.1260.

Bryn V, Verkerk R, Skjeldal OH, Saugstad OD, Ormstad H. 2017. Kynurenine pathway in autism spectrum disorders in children. Neuropsychobiology 76(2):82–88, PMID: 29694960, https://doi.org/10.1159/000488157.

Butlen-Ducuing F, Pétavy F, Guizzaro L, Zienowicz M, Salmonson T, Haas M, et al. 2016. Challenges in drug development for central nervous system disorders: a European Medicines Agency perspective. Nat Rev Drug Discov 15(12):813–814, PMID: 27895328, https://doi.org/10.1038/nrd.2016.237.

Cai J, Ding L, Zhang J-S, Xue J, Wang L-Z. 2016. Elevated plasma levels of glutamate in children with autism spectrum disorders. Neuroreport 27(4):272–276, PMID: 26825346, https://doi.org/10.1097/WNR.0000000000000532.

Cetin FH, Tunca H, Güney E, Iseri E. 2015. Neurotransmitter systems in autism spectrum disorder. In: *Autism Spectrum Disorder—Recent Advances*. Fitzgerald M, ed. London, UK: InTechOpen, 15–30.

Chaste P, Leboyer M. 2012. Autism risk factors: genes, environment, and gene–environment interactions. Dialogues Clin Neurosci 14(3):281–292, PMID: 23226953, https://doi.org/10.31887/DCNS.2012.14.3/pchaste.

Chauhan A, Chauhan V. 2006. Oxidative stress in autism. Pathophysiology 13(3):171–181, PMID: 16766163, https://doi.org/10.1016/j.pathophys.2006.05.007.

Cochran DM, Sikoglu EM, Hodge SM, Edden RAE, Foley A, Kennedy DN, et al. 2015. Relationship among glutamine, γ-aminobutyric acid, and social cognition in autism spectrum disorders. J Child Adolesc Psychopharmacol 25(4):314–322, PMID: 25919578, https://doi.org/10.1089/cap.2014.0112.

Cohen BI. 2002. The significance of ammonia/gamma-aminobutyric acid (GABA) ratio for normality and liver disorders. Med Hypotheses 59(6):757–758, PMID: 12445521, https://doi.org/10.1016/s0306-9877(02)00325-0.

Corrigan NM, Shaw DWW, Estes AM, Richards TL, Munson J, Friedman SD, et al. 2013. Atypical developmental patterns of brain chemistry in children with autism spectrum disorder. JAMA Psychiatry 70(9):964–974, PMID: 23903694, https://doi.org/10.1001/jamapsychiatry.2013.1388.

Cotney J, Muhle RA, Sanders SJ, Liu L, Willsey AJ, Niu W, et al. 2015. The autism-associated chromatin modifier CHD8 regulates other autism risk genes during human neurodevelopment. Nat Commun 6:6404, PMID: 25752243, https://doi.org/10.1038/ncomms7404.

Courchesne E, Pramparo T, Gazestani VH, Lombardo MV, Pierce K, Lewis NE. 2019. The ASD Living Biology: from cell proliferation to clinical phenotype. Mol Psychiatry 24(1):88–107, PMID: 29934544, https://doi.org/10.1038/s41380-018-0056-y.

De Felice A, Greco A, Calamandrei G, Minghetti L. 2016. Prenatal exposure to the organophosphate insecticide chlorpyrifos enhances brain oxidative stress and prostaglandin E_2 synthesis in a mouse model of idiopathic autism. J Neuroinflammation 13(1):149, PMID: 27301868, https://doi.org/10.1186/s12974-016-0617-4.

De Rubeis S, He X, Goldberg AP, Poultney CS, Samocha K, Cicek AE, et al. 2014. Synaptic, transcriptional and chromatin genes disrupted in autism. Nature 515(7526):209–215, PMID: 25363760, https://doi.org/10.1038/nature13772.

Delaye J-B, Patin F, Lagrue E, Le Tilly O, Bruno C, Vuillaume M-L, et al. 2018. Post hoc analysis of plasma amino acid profiles: towards a specific pattern in autism spectrum disorder and intellectual disability. Ann Clin Biochem 55(5):543–552, PMID: 29388433, https://doi.org/10.1177/0004563218760351.

Dhossche D, Applegate H, Abraham A, Maertens P, Bland L, Bencsath A, et al. 2002. Elevated plasma gamma-aminobutyric acid (GABA) levels in autistic youngsters: stimulus for a GABA hypothesis of autism. Med Sci Monit 8(8):PR1–PR6, PMID: 12165753.

Dietert RR, Dietert JM, Dewitt JC. 2011. Environmental risk factors for autism. Emerg Health Threats J 4:7111, PMID: 24149029, https://doi.org/10.3402/ehtj.v4i0.7111.

Drenthen GS, Barendse EM, Aldenkamp AP, van Veenendaal TM, Puts NAJ, Edden RAE, et al. 2016. Altered neurotransmitter metabolism in adolescents with high-functioning autism. Psychiatry Res Neuroimaging 256:44–49, PMID: 27685800, https://doi.org/10.1016/j.pscychresns.2016.09.007.

Eaton DL, Daroff RB, Autrup H, Bridges J, Buffler P, Costa LG, et al. 2008. Review of the toxicology of chlorpyrifos with an emphasis on human exposure and neurodevelopment. Crit Rev Toxicol 38(suppl 2):1–125, PMID: 18726789, https://doi.org/10.1080/10408440802272158.

El-Ansary A. 2016. Data of multiple regressions analysis between selected biomarkers related to glutamate excitotoxicity and oxidative stress in Saudi autistic patients. Data Brief 7:111–116, PMID: 26933667, https://doi.org/10.1016/j.dib.2016.02.025.

El-Ansary A, Al-Ayadhi L. 2014. GABAergic/glutamatergic imbalance relative to excessive neuroinflammation in autism spectrum disorders. J Neuroinflammation 11:189, PMID: 25407263, https://doi.org/10.1186/s12974-014-0189-0.

El-Ansary A, Bjørklund G, Chirumbolo S, Alnakhli OM. 2017. Predictive value of selected biomarkers related to metabolism and oxidative stress in children with autism spectrum disorder. Metab Brain Dis 32(4):1209–1221, PMID: 28497358, https://doi.org/10.1007/s11011-017-0029-x.

ElBaz FM, Zaki MM, Youssef AM, ElDorry GF, Elalfy DY. 2014. Study of plasma amino acid levels in children with autism: an Egyptian sample. Egypt J Med Hum Genet 15(2):181–186, https://doi.org/10.1016/j.ejmhg.2014.02.002.

Ernst M, Zametkin AJ, Matochik JA, Pascualvaca D, Cohen RM. 1997. Low medial prefrontal dopaminergic activity in autistic children. Lancet 350(9078):638, PMID: 9288051, https://doi.org/10.1016/s0140-6736(05)63326-0.

Evans C, Dunstan HR, Rothkirch T, Roberts TK, Reichelt KL, Cosford R, et al. 2008. Altered amino acid excretion in children with autism. Nutr Neurosci 11(1):9–17, PMID: 18510798, https://doi.org/10.1179/147683008X301360.

Fan X, Dong J, Zhong S, Wei Y, Wu Q, Yan L, et al. 2018. Spatial transcriptomic survey of human embryonic cerebral cortex by single-cell RNA-seq analysis. Cell Res 28(7):730–745, PMID: 29867213, https://doi.org/10.1038/s41422-018-0053-3.

Ford TC, Crewther DP. 2016. A comprehensive review of the ^{1}H-MRS metabolite spectrum in autism spectrum disorder. Front Mol Neurosci 9:14, PMID: 27013964, https://doi.org/10.3389/fnmol.2016.00014.

Gaetz W, Bloy L, Wang DJ, Port RG, Blaskey L, Levy SE, et al. 2014. GABA estimation in the brains of children on the autism spectrum: measurement precision and regional cortical variation. Neuroimage 86:1–9, PMID: 23707581, https://doi.org/10.1016/j.neuroimage.2013.05.068.

Gao R, Penzes P. 2015. Common mechanisms of excitatory and inhibitory imbalance in schizophrenia and autism spectrum disorders. Curr Mol Med 15(2):146–167, PMID: 25732149, https://doi.org/10.2174/1566524015666150303003028.

Gaugler T, Klei L, Sanders SJ, Bodea CA, Goldberg AP, Lee AB, et al. 2014. Most genetic risk for autism resides with common variation. Nat Genet 46(8):881–885, PMID: 25038753, https://doi.org/10.1038/ng.3039.

Geier DA, Kern JK, Garver CR, Adams JB, Audhya T, Nataf R, et al. 2009. Biomarkers of environmental toxicity and susceptibility in autism. J Neurol Sci 280(1–2):101–108, PMID: 18817931, https://doi.org/10.1016/j.jns.2008.08.021.

Gevi F, Zolla L, Gabriele S, Persico AM. 2016. Urinary metabolomics of young Italian autistic children supports abnormal tryptophan and purine metabolism. Mol Autism 7:47, PMID: 27904735, https://doi.org/10.1186/s13229-016-0109-5.

Gogolla N, Leblanc JJ, Quast KB, Südhof TC, Fagiolini M, Hensch TK. 2009. Common circuit defect of excitatory-inhibitory balance in mouse models of autism. J Neurodev Disord 1(2):172–181, PMID: 20664807, https://doi.org/10.1007/s11689-009-9023-x.

Grandjean P, Landrigan PJ. 2014. Neurobehavioural effects of developmental toxicity. Lancet Neurol 13(3):330–338, PMID: 24556010, https://doi.org/10.1016/S1474-4422(13)70278-3.

Halladay AK, Amaral D, Aschner M, Bolivar VJ, Bowman A, DiCicco-Bloom E, et al. 2009. Animal models of autism spectrum disorders: information for neurotoxicologists. Neurotoxicology 30(5):811–821, PMID: 19596370, https://doi.org/10.1016/j.neuro.2009.07.002.

Han Y, Xi Q-q, Dai W, Yang S-h, Gao L, Su Y-y, et al. 2015. Abnormal transsulfuration metabolism and reduced antioxidant capacity in Chinese children with autism spectrum disorders. Int J Dev Neurosci 46:27–32, PMID: 26150135, https://doi.org/10.1016/j.ijdevneu.2015.06.006.

Harada M, Taki MM, Nose A, Kubo H, Mori K, Nishitani H, et al. 2011. Non-invasive evaluation of the GABAergic/glutamatergic system in autistic patients observed by MEGA-editing proton MR spectroscopy using a clinical 3 Tesla instrument. J Autism Dev Disord 41(4):447–454, PMID: 20652388, https://doi.org/10.1007/s10803-010-1065-0.

Harris G, Eschment M, Orozco SP, McCaffery JM, Maclennan R, Severin D, et al. 2018. Toxicity, recovery, and resilience in a 3D dopaminergic neuronal in vitro model exposed to rotenone. Arch Toxicol 92(8):2587–2520, PMID: 29955902, https://doi.org/10.1007/s00204-018-2250-8.

Harris G, Hogberg H, Hartung T, Smirnova L. 2017. 3D differentiation of LUHMES cell line to study recovery and delayed neurotoxic effects. Curr Protoc Toxicol 73:11.23.1–11.23.28, PMID: 28777440, https://doi.org/10.1002/cptx.29.

Hartung T, Bremer S, Casati S, Coecke S, Corvi R, Fortaner S, et al. 2004. A modular approach to the ECVAM principles on test validity. Altern Lab Anim 32(5):467–472, PMID: 15656771, https://doi.org/10.1177/026119290403200503.

Hartung T, Hoffmann S, Stephens M. 2013. Mechanistic validation. ALTEX 30(2):119–130, PMID: 23665802, https://doi.org/10.14573/altex.2013.2.119.

Hassan TH, Abdelrahman HM, Fattah NRA, El-Masry NM, Hashim HM, El-Gerby KM, et al. 2013. Blood and brain glutamate levels in children with autistic disorder. Res Autism Spectr Disord 7(4):541–548, https://doi.org/10.1016/j.rasd.2012.12.005.

Hassan MH, Desoky T, Sakhr HM, Gabra RH, Bakri AH. 2019. Possible metabolic alterations among autistic male children: clinical and biochemical approaches. J Mol Neurosci 67(2):204–216, PMID: 30600432, https://doi.org/10.1007/s12031-018-1225-9.

Hérault J, Martineau J, Perrot-Beaugerie A, Jouve J, Tournade H, Barthelemy C, et al. 1993. Investigation of whole blood and urine monoamines in autism. Eur Child Adolesc Psychiatry 2(4):211–220, PMID: 29871438, https://doi.org/10.1007/BF02098580.

Horder J, Petrinovic MM, Mendez MA, Bruns A, Takumi T, Spooren W, et al. 2018. Glutamate and GABA in autism spectrum disorder—a translational magnetic resonance spectroscopy study in man and rodent models. Transl Psychiatry 8(1):106, PMID: 29802263, https://doi.org/10.1038/s41398-018-0155-1.

Howard AS, Bucelli R, Jett DA, Bruun D, Yang D, Lein PJ. 2005. Chlorpyrifos exerts opposing effects on axonal and dendritic growth in primary neuronal cultures. Toxicol Appl Pharmacol 207(2):112–124, PMID: 16102564, https://doi.org/10.1016/j.taap.2004.12.008.

Iaccarino HF, Suckow RF, Xie S, Bucci DJ. 2013. The effect of transient increases in kynurenic acid and quinolinic acid levels early in life on behavior in adulthood: implications for schizophrenia. Schizophr Res 150(2–3):392–397, PMID: 24091034, https://doi.org/10.1016/j.schres.2013.09.004.

James SJ. 2013. Autism and folate-dependent one-carbon metabolism: serendipity and critical branch-point decisions in science. Glob Adv Health Med 2(6):48–51, PMID: 24416708, https://doi.org/10.7453/gahmj.2013.088.

James SJ, Cutler P, Melnyk S, Jernigan S, Janak L, Gaylor DW, et al. 2004. Metabolic biomarkers of increased oxidative stress and impaired methylation capacity in children with autism. Am J Clin Nutr 80(6):1611–1617, PMID: 15585776, https://doi.org/10.1093/ajcn/80.6.1611.

James SJ, Melnyk S, Jernigan S, Cleves MA, Halsted CH, Wong DH, et al. 2006. Metabolic endophenotype and related genotypes are associated with oxidative stress in children with autism. Am J Med Genet B Neuropsychiatr Genet 141B(8):947–956, PMID: 16917939, https://doi.org/10.1002/ajmg.b.30366.

Joshi G, Biederman J, Wozniak J, Goldin RL, Crowley D, Furtak S, et al. 2013. Magnetic resonance spectroscopy study of the glutamatergic system in adolescent males with high-functioning autistic disorder: a pilot study at 4T. Eur Arch Psychiatry Clin Neurosci 263(5):379–384, PMID: 22986449, https://doi.org/10.1007/s00406-012-0369-9.

Juberg DR, Hoberman AM, Marty S, Picut CA, Stump DG. 2019. Letter to the editor regarding "safety of safety evaluation of pesticides: developmental neurotoxicity of chlorpyrifos and chlorpyrifos-methyl" by Mie et al. (environmental health. 2018. 17:77). Environ Health 18(1):21, PMID: 30871546, https://doi.org/10.1186/s12940-019-0454-x.

Kałużna-Czaplińska J, Jóźwik-Pruska J, Chirumbolo S, Bjørklund G. 2017. Tryptophan status in autism spectrum disorder and the influence of supplementation on its level. Metab Brain Dis 32(5):1585–1593, PMID: 28608247, https://doi.org/10.1007/s11011-017-0045-x.

Kałużna-Czaplińska J, Socha E, Rynkowski J. 2010. Determination of homovanillic acid and vanillylmandelic acid in urine of autistic children by gas chromatography/mass spectrometry. Med Sci Monit 16(9):CR445–CR450, PMID: 20802418.

Kałużna-Czaplińska J, Żurawicz E, Struck W, Markuszewski M. 2014. Identification of organic acids as potential biomarkers in the urine of autistic children using gas chromatography/mass spectrometry. J Chromatogr B Analyt Technol Biomed Life Sci 966:70–76, PMID: 24565890, https://doi.org/10.1016/j.jchromb.2014.01.041.

Kamath V, Moberg PJ, Gur RE, Doty RL, Turetsky BI. 2012. Effects of the val(158)met catechol-o-methyltransferase gene polymorphism on olfactory processing in schizophrenia. Behav Neurosci 126(1):209–215, PMID: 22148860, https://doi.org/10.1037/a0026466.

Karimi P, Kamali E, Mousavi SM, Karahmadi M. 2017. Environmental factors influencing the risk of autism. J Res Med Sci 22:27, PMID: 28413424, https://doi.org/10.4103/1735-1995.200272.

Khemakhem AM, Frye RE, El-Ansary A, Al-Ayadhi L, Bacha AB. 2017. Novel biomarkers of metabolic dysfunction is autism spectrum disorder: potential for biological diagnostic markers. Metab Brain Dis 32(6):1983–1997, PMID: 28831647, https://doi.org/10.1007/s11011-017-0085-2.

Kim JY, Son MJ, Son CY, Radua J, Eisenhut M, Gressier F, et al. 2019. Environmental risk factors and biomarkers for autism spectrum disorder: an umbrella review of the evidence. Lancet Psychiatry 6(7):590–600, PMID: 31230684, https://doi.org/10.1016/S2215-0366(19)30181-6.

Kiykim E, Zeybek CA, Zubarioglu T, Cansever S, Yalcinkaya C, Soyucen E, et al. 2016. Inherited metabolic disorders in Turkish patients with autism spectrum disorders. Autism Res 9(2):217–223, PMID: 26055667, https://doi.org/10.1002/aur.1507.

Kolodny T, Schallmo M-P, Gerdts J, Edden RAE, Bernier RA, Murray SO. 2020. Concentrations of cortical GABA and glutamate in young adults with autism spectrum disorder. Autism Res 13(7):1111–1129, PMID: 32297709, https://doi.org/10.1002/aur.2300.

Koshlukova SE, Reed NR. 2014. Chlorpyrifos. In: *Encyclopedia of Toxicology*. Wexler P, ed. 3rd ed. Amsterdam, Netherlands: Academic Press, 930–934.

Koufaris C, Sismani C. 2015. Modulation of the genome and epigenome of individuals susceptible to autism by environmental risk factors. Int J Mol Sci 16(4):8699–8718, PMID: 25903146, https://doi.org/10.3390/ijms16048699.

Kubas B, Kułak W, Sobaniec W, Tarasow E, Lebkowska U, Walecki J. 2012. Metabolite alterations in autistic children: a ^{1}H MR spectroscopy study. Adv Med Sci 57(1):152–156, PMID: 22472469, https://doi.org/10.2478/v10039-012-0014-x.

Kuwabara H, Yamasue H, Koike S, Inoue H, Kawakubo Y, Kuroda M, et al. 2013. Altered metabolites in the plasma of autism spectrum disorder: a capillary electrophoresis time-of-flight mass spectroscopy study. PLoS One 8(9):e73814, PMID: 24058493, https://doi.org/10.1371/journal.pone.0073814.

Kuwagata M, Ogawa T, Shioda S, Nagata T. 2009. Observation of fetal brain in a rat valproate-induced autism model: a developmental neurotoxicity study. Int J Dev Neurosci 27(4):399–405, PMID: 19460635, https://doi.org/10.1016/j.ijdevneu.2009.01.006.

Lachman HM. 2008. Perspective: does *COMT* val^{158}met affect behavioral phenotypes: yes, no, maybe? Neuropsychopharmacology 33(13):3027–3029, PMID: 18923401, https://doi.org/10.1038/npp.2008.189.

Lachman HM, Papolos DF, Saito T, Yu Y-M, Szumlanski CL, Weinshilboum RM. 1996. Human catechol-O-methyltransferase pharmacogenetics: description of a functional polymorphism and its potential application to neuropsychiatric disorders. Pharmacogenetics 6(3):243–250, PMID: 8807664, https://doi.org/10.1097/00008571-199606000-00007.

Lai M-C, Lombardo MV, Baron-Cohen S. 2014. Autism. Lancet 383(9920):896–910, PMID: 24074734, https://doi.org/10.1016/S0140-6736(13)61539-1.

Lancaster MA, Renner M, Martin C-A, Wenzel D, Bicknell LS, Hurles ME, et al. 2013. Cerebral organoids model human brain development and microcephaly. Nature 501(7467):373–379, PMID: 23995685, https://doi.org/10.1038/nature12517.

Landrigan PJ. 2010. What causes autism? Exploring the environmental contribution. Curr Opin Pediatr 22(2):219–225, PMID: 20087185, https://doi.org/10.1097/MOP.0b013e328336eb9a.

Landrigan PJ, Lambertini L, Birnbaum LS. 2012. A research strategy to discover the environmental causes of autism and neurodevelopmental disabilities. Environ Health Perspect 120(7):a258–a260, PMID: 22543002, https://doi.org/10.1289/ehp.1104285.

LaSalle JM. 2013. Epigenomic strategies at the interface of genetic and environmental risk factors for autism. J Hum Genet 58(7):396–401, PMID: 23677056, https://doi.org/10.1038/jhg.2013.49.

Lawrence YA, Kemper TL, Bauman ML, Blatt GJ. 2010. Parvalbumin-, calbindin-, and calretinin-immunoreactive hippocampal interneuron density in autism. Acta Neurol Scand 121(2):99–108, PMID: 19719810, https://doi.org/10.1111/j.1600-0404.2009.01234.x.

Leist M, Hasiwa N, Daneshian M, Hartung T. 2012. Validation and quality control of replacement alternatives—current status and future challenges. Toxicol Res 1(1):8–22, https://doi.org/10.1039/c2tx20011b.

Lewine JD, Andrews R, Chez M, Patil AA, Devinsky O, Smith M, et al. 1999. Magnetoencephalographic patterns of epileptiform activity in children with regressive autism spectrum disorders. Pediatrics 104(3 pt 1):405–418, PMID: 10469763, https://doi.org/10.1542/peds.104.3.405.

Li J, Settivari R, LeBaron MJ, Marty MS. 2019. An industry perspective: a streamlined screening strategy using alternative models for chemical assessment of developmental neurotoxicity. Neurotoxicology 73:17–30, PMID: 30786249, https://doi.org/10.1016/j.neuro.2019.02.010.

Limongi T, Cesca F, Gentile F, Marotta R, Ruffilli R, Barberis A, et al. 2013. Nanostructured superhydrophobic substrates trigger the development of 3D neuronal networks. Small 9(3):402–412, PMID: 23027505, https://doi.org/10.1002/smll.201201377.

Liu A, Zhou W, Qu L, He F, Wang H, Wang Y, et al. 2019. Altered urinary amino acids in children with autism spectrum disorders. Front Cell Neurosci 13:7, PMID: 30733669, https://doi.org/10.3389/fncel.2019.00007.

Lussu M, Noto A, Masili A, Rinaldi AC, Dessì A, De Angelis M, et al. 2017. The urinary ^{1}H-NMR metabolomics profile of an Italian autistic children population and their unaffected siblings. Autism Res 10(6):1058–1066, PMID: 28296209, https://doi.org/10.1002/aur.1748.

Lyall K, Croen L, Daniels J, Fallin MD, Ladd-Acosta C, Lee BK, et al. 2017. The changing epidemiology of autism spectrum disorders. Annu Rev Public Health 38:81–102, PMID: 28068486, https://doi.org/10.1146/annurev-publhealth-031816-044318.

Mandy W, Lai M-C. 2016. Annual research review: the role of the environment in the developmental psychopathology of autism spectrum condition. J Child Psychol Psychiatry 57(3):271–292, PMID: 26782158, https://doi.org/10.1111/jcpp.12501.

Mariani J, Coppola G, Zhang P, Abyzov A, Provini L, Tomasini L, et al. 2015. FOXG1-dependent dysregulation of GABA/glutamate neuron differentiation in autism spectrum disorders. Cell 162(2):375–390, PMID: 26186191, https://doi.org/10.1016/j.cell.2015.06.034.

Marotta R, Risoleo MC, Messina G, Parisi L, Carotenuto M, Vetri L, et al. 2020. The neurochemistry of autism. Brain Sci 10(3):163, PMID: 32182969, https://doi.org/10.3390/brainsci10030163.

Martineau J, Barthélémy C, Jouve J, Muh JP, LeLord G. 1992. Monoamines (serotonin and catecholamines) and their derivatives in infantile autism: age-related changes and drug effects. Dev Med Child Neurol 34(7):593–603, PMID: 1380929, https://doi.org/10.1111/j.1469-8749.1992.tb11490.x.

Martineau J, Hérault J, Petit E, Guérin P, Hameury L, Perrot A, et al. 1994. Catecholaminergic metabolism and autism. Dev Med Child Neurol 36(8):688–697, PMID: 7914177, https://doi.org/10.1111/j.1469-8749.1994.tb11911.x.

Marx U, Akabane T, Andersson TB, Baker E, Beilmann M, Beken S, et al. 2020. Biology-inspired microphysiological systems to advance patient benefit and animal welfare in drug development. ALTEX 37(3):365–394, PMID: 32113184, https://doi.org/10.14573/altex.2001241.

Marx U, Andersson TB, Bahinski A, Beilmann M, Beken S, Cassee FR, et al. 2016. Biology-inspired microphysiological system approaches to solve the prediction dilemma of substance testing. ALTEX 33(3):272–321, PMID: 27180100, https://doi.org/10.14573/altex.1603161.

Mavel S, Nadal-Desbarats L, Blasco H, Bonnet-Brilhault F, Barthélémy C, Montigny F, et al. 2013. ^{1}H–^{13}C NMR-based urine metabolic profiling in autism spectrum disorders. Talanta 114:95–102, PMID: 23953447, https://doi.org/10.1016/j.talanta.2013.03.064.

McTighe SM, Neal SJ, Lin Q, Hughes ZA, Smith DG. 2013. The BTBR mouse model of autism spectrum disorders has learning and attentional impairments and alterations in acetylcholine and kynurenic acid in prefrontal cortex. PLoS One 8(4):e62189, PMID: 23638000, https://doi.org/10.1371/journal.pone.0062189.

Melnyk S, Fuchs GJ, Schulz E, Lopez M, Kahler SG, Fussell JJ, et al. 2012. Metabolic imbalance associated with methylation dysregulation and oxidative damage in children with autism. J Autism Dev Disord 42(3):367–377, PMID: 21519954, https://doi.org/10.1007/s10803-011-1260-7.

Mie A, Rudén C, Grandjean P. 2018. Safety of safety evaluation of pesticides: developmental neurotoxicity of chlorpyrifos and chlorpyrifos-methyl. Environ Health 17(1):77, PMID: 30442131, https://doi.org/10.1186/s12940-018-0421-y.

Ming X, Stein TP, Barnes V, Rhodes N, Guo L. 2012. Metabolic perturbance in autism spectrum disorders: a metabolomics study. J Proteome Res 11(12):5856–5862, PMID: 23106572, https://doi.org/10.1021/pr300910n.

Modabbernia A, Velthorst E, Reichenberg A. 2017. Environmental risk factors for autism: an evidence-based review of systematic reviews and meta-analyses. Mol Autism 8:13, PMID: 28331572, https://doi.org/10.1186/s13229-017-0121-4.

Mohs RC, Greig NH. 2017. Drug discovery and development: role of basic biological research. Alzheimers Dement (NY) 3(4):651–657, PMID: 29255791, https://doi.org/10.1016/j.trci.2017.10.005.

Moreno-Fuenmayor H, Borjas L, Arrieta A, Valera V, Socorro-Candanoza L. 1996. Plasma excitatory amino acids in autism. Invest Clin 37(2):113–128, PMID: 8718922.

Murakami Y, Imamura Y, Saito K, Sakai D, Motoyama J. 2019. Altered kynurenine pathway metabolites in a mouse model of human attention-deficit hyperactivity/autism spectrum disorders: a potential new biological diagnostic marker. Sci Rep 9(1):13182, PMID: 31515500, https://doi.org/10.1038/s41598-019-49781-y.

Nadal-Desbarats L, Aïdoud N, Emond P, Blasco H, Filipiak I, Sarda P, et al. 2014. Combined ^{1}H-NMR and ^{1}H–^{13}C HSQC-NMR to improve urinary screening in autism spectrum disorders. Analyst 139(13):3460–3468, PMID: 24841505, https://doi.org/10.1039/c4an00552j.

Naushad SM, Jain JMN, Prasad CK, Naik U, Akella RRD. 2013. Autistic children exhibit distinct plasma amino acid profile. Indian J Biochem Biophys 50(5):474–478, PMID: 24772971.

Neale BM, Kou Y, Liu L, Ma'ayan A, Samocha KE, Sabo A, et al. 2012. Patterns and rates of exonic *de novo* mutations in autism spectrum disorders. Nature 485(7397):242–245, PMID: 22495311, https://doi.org/10.1038/nature11011.

Noto A, Fanos V, Barberini L, Grapov D, Fattuoni C, Zaffanello M, et al. 2014. The urinary metabolomics profile of an Italian autistic children population and their unaffected siblings. J Maternal-Fetal Neonatal Med 27(suppl 2):46–52, PMID: 25284177, https://doi.org/10.3109/14767058.2014.954784.

OECD (Organisation for Economic Co-operation and Development). 1997. Neurotoxicity study in rodents. OECD Guideline for Testing of Chemicals, No. 424. Paris, France: OECD. https://www.oecd-ilibrary.org/test-no-424-neurotoxicity-2study-in-rodents_5lmqcr2k7mwj.pdf?itemId=%2Fcontent%2Fpublication%2F9789264071025-en [accessed 16 June 2021].

OECD. 2007. Developmental neurotoxicity study. OECD Guideline for Testing of Chemicals, No. 426. Paris, France: OECD. https://www.oecd.org/chemicalsafety/testing/37622194.pdf [accessed 16 June 2021].

OECD. 2018. Extended one-generation reproductive toxicity study. OECD Guideline for Testing of Chemicals, No. 443. Paris, France: OECD. https://www.oecd.org/chemicalsafety/test-no-443-extended-one-generation-reproductive-toxicity-study-9789264185371-en.htm [accessed 16 June 2021].

Orekhova EV, Stroganova TA. 2014. Arousal and attention re-orienting in autism spectrum disorders: evidence from auditory event-related potentials. Front Hum Neurosci 8:34, PMID: 24567709, https://doi.org/10.3389/fnhum.2014.00034.

Ormstad H, Bryn V, Verkerk R, Skjeldal OH, Halvorsen B, Saugstad OD, et al. 2018. Serum tryptophan, tryptophan catabolites and brain-derived neurotrophic factor in subgroups of youngsters with autism spectrum disorders. CNS Neurological Disord Drug Targets 17(8):626–639, PMID: 30033880, https://doi.org/10.2174/1871527317666180720163221.

Orozco JS, Hertz-Picciotto I, Abbeduto L, Slupsky CM. 2019. Metabolomics analysis of children with autism, idiopathic-developmental delays, and Down syndrome. Transl Psychiatry 9(1):243, PMID: 31582732, https://doi.org/10.1038/s41398-019-0578-3.

Pamies D, Barreras P, Block K, Makri G, Kumar A, Wiersma D, et al. 2017. A human brain microphysiological system derived from induced pluripotent stem cells to study neurological diseases and toxicity. ALTEX 34(3):362–376, PMID: 27883356, https://doi.org/10.14573/altex.1609122.

Pamies D, Block K, Lau P, Gribaldo L, Pardo CA, Barreras P, et al. 2018. Rotenone exerts developmental neurotoxicity in a human brain spheroid model. Toxicol Appl Pharmacol 354:101–114, PMID: 29428530, https://doi.org/10.1016/j.taap.2018.02.003.

Pamies D, Hartung T. 2017. 21st century cell culture for 21st century toxicology. Chem Res Toxicol 30(1):43–52, PMID: 28092941, https://doi.org/10.1021/acs.chemrestox.6b00269.

Pavăl D. 2017. A dopamine hypothesis of autism spectrum disorder. Dev Neurosci 39(5):355–360, PMID: 28750400, https://doi.org/10.1159/000478725.

Peretz H, Talpalar AE, Vago R, Baranes D. 2007. Superior survival and durability of neurons and astrocytes on 3-dimensional aragonite biomatrices. Tissue Eng 13(3):461–472, PMID: 17319796, https://doi.org/10.1089/ten.2005.0522.

Persico AM, Napolioni V. 2013. Autism genetics. Behav Brain Res 251:95–112, PMID: 23769996, https://doi.org/10.1016/j.bbr.2013.06.012.

Peter CJ, Reichenberg A, Akbarian S. 2015. Epigenetic regulation in autism. In: *The Molecular Basis of Autism*. Fatemi S, ed. New York, NY: Springer, 67–92.

Pistollato F, Ohayon EL, Lam A, Langley GR, Novak TJ, Pamies D, et al. 2016. Alzheimer disease research in the 21st century: past and current failures, new perspectives and funding priorities. Oncotarget 7(26):38999–39016, PMID: 27229915, https://doi.org/10.18632/oncotarget.9175.

Platt RJ, Zhou Y, Slaymaker IM, Shetty AS, Weisbach NR, Kim J-A, et al. 2017. *Chd8* mutation leads to autistic-like behaviors and impaired striatal circuits. Cell Rep 19(2):335–350, PMID: 28402856, https://doi.org/10.1016/j.celrep.2017.03.052.

Ramos-Chávez LA, Huitrón RL, Esquivel DG, Pineda B, Ríos C, Silva-Adaya D, et al. 2018. Relevance of alternative routes of kynurenic acid production in the brain.

Oxid Med Cell Longev 2018:5272741, PMID: 29977455, https://doi.org/10.1155/2018/5272741.
Rauh V, Arunajadai S, Horton M, Perera F, Hoepner L, Barr DB, et al. 2011. Seven-year neurodevelopmental scores and prenatal exposure to chlorpyrifos, a common agricultural pesticide. Environ Health Perspect 119(8):1196–1201, PMID: 21507777, https://doi.org/10.1289/ehp.1003160.
Rauh VA, Garfinkel R, Perera FP, Andrews HF, Hoepner L, Barr DB, et al. 2006. Impact of prenatal chlorpyrifos exposure on neurodevelopment in the first 3 years of life among inner-city children. Pediatrics 118(6):e1845–e1859, PMID: 17116700, https://doi.org/10.1542/peds.2006-0338.
Rauh VA, Perera FP, Horton MK, Whyatt RM, Bansal R, Hao X, et al. 2012. Brain anomalies in children exposed prenatally to a common organophosphate pesticide. Proc Natl Acad Sci USA 109(20):7871–7876, PMID: 22547821, https://doi.org/10.1073/pnas.1203396109.
Rice D, Barone S Jr. 2000. Critical periods of vulnerability for the developing nervous system: evidence from humans and animal models. Environ Health Perspect 108(suppl 3):511–533, PMID: 10852851, https://doi.org/10.1289/ehp.00108s3511.
Rippon G, Brock J, Brown C, Boucher J. 2007. Disordered connectivity in the autistic brain: challenges for the 'new psychophysiology.' Int J Psychophysiol 63(2):164–172, PMID: 16820239, https://doi.org/10.1016/j.ijpsycho.2006.03.012.
Rojas DC, Singel D, Steinmetz S, Hepburn S, Brown MS. 2014. Decreased left perisylvian GABA concentration in children with autism and unaffected siblings. Neuroimage 86:28–34, PMID: 23370056, https://doi.org/10.1016/j.neuroimage.2013.01.045.
Rossignol DA, Genuis SJ, Frye RE. 2014. Environmental toxicants and autism spectrum disorders: a systematic review. Transl Psychiatry 4(2):e360, PMID: 24518398, https://doi.org/10.1038/tp.2014.4.
Rubenstein JLR, Merzenich MM. 2003. Model of autism: increased ratio of excitation/inhibition in key neural systems. Genes Brain Behav 2(5):255–267, PMID: 14606691, https://doi.org/10.1034/j.1601-183x.2003.00037.x.
Rylaarsdam L, Guemez-Gamboa A. 2019. Genetic causes and modifiers of autism spectrum disorder. Front Cell Neurosci 13:385, PMID: 31481879, https://doi.org/10.3389/fncel.2019.00385.
Saleem TH, Shehata GA, Toghan R, Sakhr HM, Bakri AH, Desoky T, et al. 2020. Assessments of amino acids, ammonia and oxidative stress among cohort of Egyptian autistic children: correlations with electroencephalogram and disease severity. Neuropsychiatr Dis Treat 16:11–24, PMID: 32021195, https://doi.org/10.2147/NDT.S233105.
Sanders SJ. 2015. First glimpses of the neurobiology of autism spectrum disorder. Curr Opin Genet Dev 33:80–92, PMID: 26547130, https://doi.org/10.1016/j.gde.2015.10.002.
Sanders SJ, He X, Willsey AJ, Ercan-Sencicek AG, Samocha KE, Cicek AE, et al. 2015. Insights into autism spectrum disorder genomic architecture and biology from 71 risk loci. Neuron 87(6):1215–1233, PMID: 26402605, https://doi.org/10.1016/j.neuron.2015.09.016.
Sandin S, Lichtenstein P, Kuja-Halkola R, Larsson H, Hultman CM, Reichenberg A. 2014. The familial risk of autism. JAMA 311(17):1770–1777, PMID: 24794370, https://doi.org/10.1001/jama.2014.4144.
Satterstrom FK, Kosmicki JA, Wang J, Breen MS, De Rubeis S, An J-Y, et al. 2020. Large-scale exome sequencing study implicates both developmental and functional changes in the neurobiology of autism. Cell 180(3):568–584.e23, PMID: 31981491, https://doi.org/10.1016/j.cell.2019.12.036.
Schaevitz LR, Berger-Sweeney JE. 2012. Gene–environment interactions and epigenetic pathways in autism: the importance of one-carbon metabolism. ILAR J 53(3–4):322–340, PMID: 23744970, https://doi.org/10.1093/ilar.53.3-4.322.
Scharfman HE, Goodman JH, Schwarcz R. 2000. Electrophysiological effects of exogenous and endogenous kynurenic acid in the rat brain: studies *in vivo* and *in vitro*. Amino Acids 19(1):283–297, PMID: 11026500, https://doi.org/10.1007/s007260070060.
Schmidt RJ, Hansen RL, Hartiala J, Allayee H, Schmidt LC, Tancredi DJ, et al. 2011. Prenatal vitamins, one-carbon metabolism gene variants, and risk for autism. Epidemiology 22(4):476–485, PMID: 21610500, https://doi.org/10.1097/EDE.0b013e31821d0e30.
Schneider CA, Rasband WS, Eliceiri KW. 2012. NIH image to ImageJ: 25 years of image analysis. Nat Methods 9(7):671–675, PMID: 22930834, https://doi.org/10.1038/nmeth.2089.
Shelton JF, Geraghty EM, Tancredi DJ, Delwiche LD, Schmidt RJ, Ritz B, et al. 2014. Neurodevelopmental disorders and prenatal residential proximity to agricultural pesticides: the CHARGE study. Environ Health Perspect 122(10):1103–1109, PMID: 24954055, https://doi.org/10.1289/ehp.1307044.
Shimmura C, Suda S, Tsuchiya KJ, Hashimoto K, Ohno K, Matsuzaki H, et al. 2011. Alteration of plasma glutamate and glutamine levels in children with high-functioning autism. PLoS One 6(10):e25340, PMID: 21998651, https://doi.org/10.1371/journal.pone.0025340.
Shinohe A, Hashimoto K, Nakamura K, Tsujii M, Iwata Y, Tsuchiya KJ, et al. 2006. Increased serum levels of glutamate in adult patients with autism. Prog Neuropsychopharmacol Biol Psychiatry 30(8):1472–1477, PMID: 16863675, https://doi.org/10.1016/j.pnpbp.2006.06.013.
Sillé FCM, Karakitsios S, Kleensang A, Koehler K, Maertens A, Miller GW, et al. 2020. The exposome—a new approach for risk assessment. ALTEX 37(1):3–23, PMID: 31960937, https://doi.org/10.14573/altex.2001051.
Simpson EH, Morud J, Winiger V, Biezonski D, Zhu JP, Bach ME, et al. 2014. Genetic variation in COMT activity impacts learning and dopamine release capacity in the striatum. Learn Mem 21(4):205–214, PMID: 24639487, https://doi.org/10.1101/lm.032094.113.
Slotkin TA, Seidler FJ. 2010. Oxidative stress from diverse developmental neurotoxicants: antioxidants protect against lipid peroxidation without preventing cell loss. Neurotoxicol Teratol 32(2):124–131, PMID: 20004241, https://doi.org/10.1016/j.ntt.2009.12.001.
Smirnova L, Hogberg HT, Leist M, Hartung T. 2014. Developmental neurotoxicity—challenges in the 21st century and in vitro opportunities. ALTEX 31(2):129–156, PMID: 24687333, https://doi.org/10.14573/altex.1403271.
Smith AM, King JJ, West PR, Ludwig MA, Donley ELR, Burrier RE, et al. 2019. Amino acid dysregulation metabotypes: potential biomarkers for diagnosis and individualized treatment for subtypes of autism spectrum disorder. Biol Psychiatry 85(4):345–354, PMID: 30446206, https://doi.org/10.1016/j.biopsych.2018.08.016.
Stamou M, Streifel KM, Goines PE, Lein PJ. 2013. Neuronal connectivity as a convergent target of gene × environment interactions that confer risk for autism spectrum disorders. Neurotoxicol Teratol 36:3–16, PMID: 23269408, https://doi.org/10.1016/j.ntt.2012.12.001.
Stolerman ES, Smith B, Chaubey A, Jones JR. 2016. *CHD8* intragenic deletion associated with autism spectrum disorder. Eur J Med Genet 59(4):189–194, PMID: 26921529, https://doi.org/10.1016/j.ejmg.2016.02.010.
Suetterlin P, Hurley S, Mohan C, Riegman KLH, Pagani M, Caruso A, et al. 2018. Altered neocortical gene expression, brain overgrowth and functional over-connectivity in *Chd8* haploinsufficient mice. Cereb Cortex 28(6):2192–2206, PMID: 29668850, https://doi.org/10.1093/cercor/bhy058.
Sugathan A, Biagioli M, Golzio C, Erdin S, Blumenthal I, Manavalan P, et al. 2014. *CHD8* regulates neurodevelopmental pathways associated with autism spectrum disorder in neural progenitors. Proc Natl Acad Sci USA 111(42):E4468–E4477, PMID: 25294932, https://doi.org/10.1073/pnas.1405266111.
Tirouvanziam R, Obukhanych TV, Laval J, Aronov PA, Libove R, Banerjee AG, et al. 2012. Distinct plasma profile of polar neutral amino acids, leucine, and glutamate in children with autism spectrum disorders. J Autism Dev Disord 42(5):827–836, PMID: 21713591, https://doi.org/10.1007/s10803-011-1314-x.
Torres-Altoro MI, Mathur BN, Drerup JM, Thomas R, Lovinger DM, O'Callaghan JP, et al. 2011. Organophosphates dysregulate dopamine signaling, glutamatergic neurotransmission, and induce neuronal injury markers in striatum. J Neurochem 119(2):303–313, PMID: 21848865, https://doi.org/10.1111/j.1471-4159.2011.07428.x.
Tu W-J, Chen H, He J. 2012. Application of LC-MS/MS analysis of plasma amino acids profiles in children with autism. J Clin Biochem Nutr 51(3):248–249, PMID: 23170055, https://doi.org/10.3164/jcbn.12-45.
van Elst LT, Maier S, Fangmeier T, Endres D, Mueller GT, Nickel K, et al. 2014. Disturbed cingulate glutamate metabolism in adults with high-functioning autism spectrum disorder: evidence in support of the excitatory/inhibitory imbalance hypothesis. Mol Psychiatry 19(12):1314–1325, PMID: 25048006, https://doi.org/10.1038/mp.2014.62.
van Schaftingen E, Rzem R, Veiga-da-Cunha M. 2009. L-2-Hydroxyglutaric aciduria, a disorder of metabolite repair. J Inherit Metab Dis 32(2):135–142, PMID: 19020988, https://doi.org/10.1007/s10545-008-1042-3.
Vohra M, Lemieux GA, Lin L, Ashrafi K. 2018. Kynurenic acid accumulation underlies learning and memory impairment associated with aging. Genes Dev 32(1):14–19, PMID: 29386332, https://doi.org/10.1101/gad.307918.117.
Vorstman JAS, Parr JR, Moreno-De-Luca D, Anney RJL, Nurnberger JI Jr, Hallmayer JF. 2017. Autism genetics: opportunities and challenges for clinical translation. Nat Rev Genet 18(6):362–376, PMID: 28260791, https://doi.org/10.1038/nrg.2017.4.
Wang P, Lin M, Pedrosa E, Hrabovsky A, Zhang Z, Guo W, et al. 2015. CRISPR/Cas9-mediated heterozygous knockout of the autism gene *CHD8* and characterization of its transcriptional networks in neurodevelopment. Mol Autism 6:55, PMID: 26491539, https://doi.org/10.1186/s13229-015-0048-6.
Wang P, Mokhtari R, Pedrosa E, Kirschenbaum M, Bayrak C, Zheng D, et al. 2017. CRISPR/Cas9-mediated heterozygous knockout of the autism gene CHD8 and characterization of its transcriptional networks in cerebral organoids derived from iPS cells. Mol Autism 8:11, PMID: 28321286, https://doi.org/10.1186/s13229-017-0124-1.
West PR, Amaral DG, Bais P, Smith AM, Egnash LA, Ross ME, et al. 2014. Metabolomics as a tool for discovery of biomarkers of autism spectrum disorder in the blood plasma of children. PLoS One 9(11):e112445, PMID: 25380056, https://doi.org/10.1371/journal.pone.0112445.

Wheeler AR. 2019. Administrator, U.S. Environmental Protection Agency to Associate Deputy Administrator, General Counsel, Assistant Administrators, Inspector General, Chief Financial Officer, Chief of Staff, Associate Administrators, Regional Administrators. Directive to Prioritize Efforts to Reduce Animal Testing. 10 September 2019. Washington, DC: U.S. Environmental Protection Agency. https://www.epa.gov/sites/production/files/2019-09/documents/image2019-09-09-231249.pdf [accessed 2 June 2021].

Willsey AJ, Sanders SJ, Li M, Dong S, Tebbenkamp AT, Muhle RA, et al. 2013. Coexpression networks implicate human midfetal deep cortical projection neurons in the pathogenesis of autism. Cell 155(5):997–1007, PMID: 24267886, https://doi.org/10.1016/j.cell.2013.10.020.

Yang D, Howard A, Bruun D, Ajua-Alemanj M, Pickart C, Lein PJ. 2008. Chlorpyrifos and chlorpyrifos-oxon inhibit axonal growth by interfering with the morphogenic activity of acetylcholinesterase. Toxicol Appl Pharmacol 228(1):32–41, PMID: 18076960, https://doi.org/10.1016/j.taap.2007.11.005.

Yang G, Shcheglovitov A. 2020. Probing disrupted neurodevelopment in autism using human stem cell-derived neurons and organoids: an outlook into future diagnostics and drug development. Dev Dyn 249(1):6–33, PMID: 31398277, https://doi.org/10.1002/dvdy.100.

Yap IKS, Angley M, Veselkov KA, Holmes E, Lindon JC, Nicholson JK. 2010. Urinary metabolic phenotyping differentiates children with autism from their unaffected siblings and age-matched controls. J Proteome Res 9(6):2996–3004, PMID: 20337404, https://doi.org/10.1021/pr901188e.

Yerys BE, Wallace GL, Harrison B, Celano MJ, Giedd JN, Kenworthy LE. 2009. Set-shifting in children with autism spectrum disorders: reversal shifting deficits on the Intradimensional/Extradimensional Shift Test correlate with repetitive behaviors. Autism 13(5):523–538, PMID: 19759065, https://doi.org/10.1177/1362361309335716.

Zafeiriou DI, Ververi A, Salomons GS, Vargiami E, Haas D, Papadopoulou V, et al. 2008. L-2-Hydroxyglutaric aciduria presenting with severe autistic features. Brain Dev 30(4):305–307, PMID: 17981416, https://doi.org/10.1016/j.braindev.2007.09.005.

Zhang J, Dai H, Deng Y, Tian J, Zhang C, Hu Z, et al. 2015. Neonatal chlorpyrifos exposure induces loss of dopaminergic neurons in young adult rats. Toxicology 336:17–25, PMID: 26215101, https://doi.org/10.1016/j.tox.2015.07.014.

Zheng Z, Zhu T, Qu Y, Mu D. 2016. Blood glutamate levels in autism spectrum disorder: a systematic review and meta-analysis. PLoS One 11(7):e0158688, PMID: 27390857, https://doi.org/10.1371/journal.pone.0158688.

Zhong X, Harris G, Smirnova L, Zufferey V, Sá RCDSE, Baldino Russo F, et al. 2020. Antidepressant paroxetine exerts developmental neurotoxicity in an iPSC-Derived 3D human brain model. Front Cell Neurosci 14:493, PMID: 32153365, https://doi.org/10.3389/fncel.2020.00025.